## ABSTRACT

**ROSSNER CAMPOS, ALFRED ARMIN.** Adsorption of methyl tertiary-butyl ether on high-silica zeolites: Effects of adsorbent characteristics and natural organic matter on adsorption isotherms. (Under the direction of Dr. Detlef R. U. Knappe).

Methyl *tertiary*-butyl ether (MTBE) is frequently detected in surface and ground water. Because of its hydrophilicity, MTBE is difficult to remove from aqueous solution by activated carbon adsorption processes. In drinking water treatment applications, natural organic matter (NOM) also adsorbs on activated carbons, which further decreases the MTBE adsorption capacity. Unlike activated carbons, high-silica zeolites are adsorbents with well-defined pore sizes. From a drinking water treatment perspective, it may be possible to select high-silica zeolites with pore sizes that are suitable for the adsorption of smaller organic contaminants while preventing the adsorption of competing NOM components of larger molecular size. Therefore, the objectives of this research were to evaluate the effects of zeolite pore structure and hydrophobicity on the adsorption of MTBE in the presence of NOM.

MTBE adsorption isotherm data were collected for a matrix of high-silica zeolites with different pore sizes (ZSM-5/silicalite, Mordenite, Beta, Y), exchangeable cations ($H^+$, $Na^+$, $NH_4^+$), and hydrophobicities ($SiO_2/Al_2O_3$ ratios). MTBE adsorption capacities of high-silica zeolites were compared to those of three GACs (one coconut-shell-based, two coal-based) and a carbonaceous resin (Ambersorb 563). Single-solute isotherm tests were conducted in

ultrapure water buffered at pH 7.2. Additional isotherm studies were conducted to determine the effects of co-adsorbing and preloaded NOM on MTBE adsorption from Tar River water (Greenville, NC).

Single-solute MTBE adsorption isotherm data showed that high-silica zeolites with smaller pores (ZSM-5/silicalite, Mordenite) were more effective adsorbents for MTBE than zeolites with somewhat larger pores (Beta, Y). Over a range of 90-700, the $SiO_2/Al_2O_3$ ratio of the tested ZSM-5 zeolites had no effect on MTBE adsorption capacity. Similarly, the exchangeable cation ($H^+$, $Na^+$, $NH_4^+$) of high-silica ZSM-5 zeolites had little effect on MTBE adsorption at the tested conditions, and no zeolite-catalyzed MTBE hydrolysis was apparent for ZSM-5 zeolites in the $H^+$ form.

For high-silica zeolites, co-adsorbing and preloaded NOM lowered the single-solute MTBE adsorption capacity at a liquid-phase MTBE concentration of 10 µg/L ($q_{10}$) by 0-23%. Similar decreases in MTBE adsorption capacity as a result of NOM adsorption were measured for the coconut-shell-based activated carbon CC-602; however, its MTBE adsorption capacity ($q_{10}$) was only about 25% of that obtained for ZSM-5 zeolites. In the presence of preloaded NOM, the MTBE adsorption capacity of the carbonaceous resin ($q_{10}$) decreased by about 47% relative to the single-solute value while that of one coal-based activated carbon decreased by almost 60%. Overall, the coal-based activated carbons exhibited the smallest MTBE adsorption capacities ($q_{10}$), which were approximately one order of magnitude lower than those of the ZSM-5 zeolites.

Using an equilibrium model, adsorbent usage rates (AURs) and costs associated with adsorbent usage were calculated to evaluate the feasibility of zeolite-based adsorption systems. The latter analysis showed that the lowest treatment cost ($0.7/1000 gal) was associated with the usage of HiSiv3000 zeolite (cost: ~$7/lb) and CC-602 GAC (cost: ~1.50/lb). Despite the similar cost for these two adsorbents, the zeolite-based adsorption system may be more advantageous because (1) the AUR calculated for the HiSiv3000 zeolite was less than 25% of that calculated for the CC-602 GAC and (2) the calculated bed life for a packed bed adsorber containing HiSiv3000 zeolite was more than 6 times longer than that for an equally sized packed bed adsorber containing CC-602 GAC, a result that was affected by the lower packed bed density of the latter adsorbent. Thus, adsorbent replacement/ regeneration would have to occur on a less frequent basis when zeolites are used. Finally, it may be possible to regenerate spent high-silica zeolite with steam or microwave methods rather than with more energy-intensive thermal methods. This opportunity could further lower the cost of zeolite-based adsorption systems for MTBE removal from water.

# ADSORPTION OF METHYL *TERTIARY*-BUTYL ETHER ON HIGH-SILICA ZEOLITES: EFFECTS OF ADSORBENT CHARACTERISTICS AND NATURAL ORGANIC MATTER ON ADSORPTION ISOTHERMS

**by**

**ALFRED ARMIN ROSSNER CAMPOS**

A thesis submitted to the Graduate Faculty of
North Carolina State University
in partial fulfillment of the
requirements for the Degree of
Master of Science

**CIVIL, CONSTRUCTION, AND ENVIRONMENTAL ENGINEERING**

Raleigh

2004

**APPROVED BY:**

_____

Dr. Joel Ducoste

_____

Dr. Morton Barlaz

_____

Dr. Detlef R.U. Knappe

Chair of Advisory Comitee

## BIOGRAPHY

Alfred Armin Rossner Campos was born on December 8, 1973 in Concepción, Chile. He is the son of Roberto Rossner and Carmen Campos. He has 5 siblings: 4 brothers and 1 sister. He graduated from the German school of Concepción-Chile in 1991. He received his Degree of Licentiate of Engineering Sciences in 1996 and graduated in July 1999 with a B.S. in Chemical Engineering from the University of Concepción-Chile. After graduating, Alfred worked as a research assistant in the Laboratory of Renewable Resources, University of Concepción, Chile.

In August 2002, Alfred came to the United States and began his Master of Science studies in the Department of Civil, Construction, and Environmental Engineering at North Carolina State University. Over the last two years, he has been working as a Research Assistant.

## ACKNOWLEDGEMENTS

First, I would to thank my advisor, Dr. Detlef R. U. Knappe, for his constant support and guidance throughout this research.

I will like to thank AWWA Research Foundation for sponsoring this research through project 2905. I also want to acknowledge David Black for the GC analyses.

Finally, I want to extend my gratitude to my wife Carolina and my parents whose unconditional love and support helped me achieve my goals.

**TABLE OF CONTENTS**

**List of Tables**

**List of Figures**

## 1. INTRODUCTION, HYPOTHESES, AND OBJECTIVES

Methyl tertiary-butyl ether (MTBE) is a fuel additive that serves as an octane enhancer and promotes more complete burning of gasoline. MTBE is added to about 30% of the gasoline sold in the US, and about 40% of the US population lives in areas where MTBE is used [USGS 1996]. Leaking underground storage tanks, exhausts from recreational watercrafts, and air deposition are among the sources of MTBE contamination in ground and surface waters. Because of its high solubility in water and its small molecular size, MTBE migrates rapidly in ground water aquifers, and an increasing number of public and private wells have been contaminated with MTBE as a result [EPA 1997]. Significant quantities of MTBE are allready present in the environment and may impact drinking water sources over at least the next decade [Johnson et al. 2000].

MTBE has received increasing attention in the drinking water industry because (1) it is a potential carcinogen, (2) it can adversely affect the taste and odor quality of water, and (3) it is difficult to remove from water. The removal of MTBE from drinking water is difficult to accomplish by activated carbon adsorption and air stripping because of its high water solubility and low volatility. In addition, MTBE is fairly resistant to biodegradation and chemical oxidation, and these processes may lead to the formation of undesirable metabolites or oxidation byproducts such as tertiary-butyl alcohol (TBA) or bromate [Mormile et al. 1994, Leitner et al. 1994, Liang et al. 1999]. Recently published data [Anderson 2000, Li et al. 2003a] showed that high-silica zeolites exhibit considerably larger single-solute MTBE adsorption capacities than activated carbon. However, the effects of natural organic matter

(NOM) on the MTBE adsorption capacity of high-silica zeolites are not known. Based on the existing evidence, the following hypotheses were formulated for this research:

- High-silica zeolites are more effective for MTBE removal from drinking water than carbonaceous resins and activated carbons because zeolites, with their uniform intracrystalline pore structure, can be selected such that the entire internal pore volume has the appropriate size for MTBE adsorption from aqueous solution.
- High-silica zeolites are more resistant to fouling by natural organic matter (NOM) because the well-defined pore structure of high-silica zeolites precludes NOM access to zeolite pores.

The overall objective of this research was to evaluate the effectiveness of high-silica zeolites for the removal of MTBE from drinking water. To test the above hypotheses, this research had the following specific objectives:

- Determine zeolite characteristics (pore size, $SiO_2/Al_2O_3$ ratio, and exchangeable cation) that are most suitable for the adsorption of MTBE from water,
- Compare MTBE adsorption capacities of high-silica zeolites to those of a carbonaceous resin and three activated carbons, and
- Determine the effects of co-adsorbing and preloaded NOM on MTBE adsorption capacities.
- Utilize MTBE adsorption isotherm data for a preliminary cost analysis to assess the feasibility of using zeolite-based adsorption systems for MTBE removal.

## 2. BACKGROUND

### 2.1. Methyl tertiary-butyl ether (MTBE)

MTBE was originally introduced in the U.S. fuel supply in the late 1970s to replace the octane-enhancing compound tetraethyl lead. Implementation of the Clean Air Act Amendments of 1990 led to increased use of MTBE to meet the oxygen content requirements for oxygenated and reformulated gasoline in metropolitan areas with high ambient air levels of carbon monoxide (CO) and/or ozone ($O_3$) [U.S. EPA, 2003]. In recent years, MTBE has been the fuel oxygenate most commonly used in reformulated gasoline (RFG), which is used year-round in cities trying to meet ozone ambient air standards. While other EPA-approved fuel oxygenates are available [e.g., ethyl tertiary-butyl ether (ETBE), tertiary-amyl methyl ether (TAME), diisopropyl ether (DIPE), methanol, ethanol, and tertiary-butyl alcohol (TBA)]), MTBE is added to about 85% of RFG across the US [Deeb et al. 2003]. In 1998, MTBE was the fourth-largest produced organic chemical in the US, and US MTBE consumption exceeded 10.5 mgd [Johnson et al. 2000].

Widespread MTBE use has led to frequent MTBE detections in surface and ground waters across the US. MTBE sources include gasoline leaking from underground fuel-storage tanks, urban runoff, and water craft [Squillace et al. 1997], and leaking underground storage tanks have been identified as the largest source of MTBE in subsurface environments [Deeb et al. 2003]. A recent report (October 2003) by the Environmental Working Group identified MTBE contamination in water supplies of more than 1,500 water systems in 27 states. Nearly

half exhibited MTBE levels higher than 2 μg/L, a concentration at which MTBE odor can be detected by some consumers [AWWA E-MainStream, 2004]. A US Geological Survey study found that 55% of large, urban water systems have detected MTBE in their water supplies [AWWA E-MainStream, 2004]. Also, 5% of the nationwide groundwater samples collected by the National Water-Quality Assessment Program (Nawqa) showed detectable levels of MTBE, with higher frequency in RFG areas [Lichtblau et al. 2004]. Negative publicity associated with frequent detections of MTBE in US waters has led to MTBE bans in California and other states. As a result MTBE production/use is decreasing in the US while production/use of the alternative fuel oxygenate ethanol is increasing [Lamberth 2004].

Several studies have been conducted to measure the carcinogenicity and taste and odor impacts of MTBE. MTBE was shown to cause cancer in rats and mice, which led some experts to conclude that MTBE poses a possible or potential cancer risk to humans [California EPA, 1999; Interagency Oxygenated Fuels Assessment Steering Committee, 1997; U.S. EPA, 1994a]. However, other studies concluded that there is not enough information to classify MTBE as a human carcinogen [U.S. Department of Health and Human Services, 2002; World Health Organization, 1998]. The odor threshold for MTBE in water is 34 μg/L (geometric mean value obtained with an expert panel, Young et al. 1996). However, a follow-up study conducted with a consumer panel yielded a geometric mean value for the threshold odor concentration of 15 μg/L [Stocking et al. 2001]. Based on the available health data, the U.S. Environmental Protection Agency (US EPA) has not set a health-based maximum contaminant level for MTBE. However, it did issue a drinking water advisory for MTBE concentrations of 20-40 μg/L based on the expert panel odor data [U.S.

EPA, 1997]. The California EPA [California EPA, 1999] set a primary health-based MTBE standard of 13 μg/L and a secondary MTBE standard based on taste and odor properties of 5 μg/L. The latter standard is enforceable in California.

Due to its high water solubility, low Henry's law constant, small molecular size, and relative biorecalcitrance, MTBE is comparatively persistent in the environment [Squillace et al. 1997] and can move quickly and farther in water than other toxic components of gasoline. The high aqueous solubility and low volatility of MTBE (Table 1) make MTBE relatively difficult to remove from water with treatment processes such as air stripping and activated carbon adsorption. In addition, biodegradation and chemical oxidation of MTBE may lead to the formation of undesirable metabolites or oxidation byproducts such as tertiary-butyl alcohol (TBA) or bromate [Mormile et al. 1994, Leitner et al. 1994, Liang et al. 1999, Acero et al. 2001].

**Table 1. Physicochemical properties and molecular structure of MTBE [U.S. EPA, 1994b, Li et al. 2002]**

| | | |
|---|---|---|
| Molecular Weight (g/mol) | 88.15 | 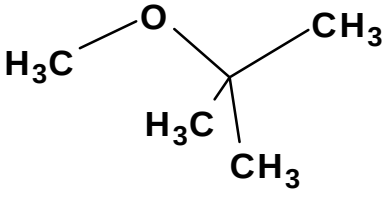 |
| Aqueous Solubility at 25°C (g/L) | 51.26 | |
| Log $K_{OW}$ | 1.24 | |
| Henry's Law Constant at 25°C ($atm \cdot m^3/mol$) | $5.5 \cdot 10^{-4}$ | |

## 2.2. Treatment options for MTBE removal

MTBE removal from water can be achieved by processes such as air stripping, adsorption, advanced oxidation, membrane separation, phytoremediation, and biological degradation [Deeb et al. 2003, Shih et al. 2003, Ramakrishnan et al. 2004, Sutherland et al. 2004]. Air stripping can be an effective process for MTBE removal; however, low mass transfer coefficients are observed for these systems due to the low volatility and high water solubility of MTBE. Consequently, relatively tall packed towers are required to achieve high MTBE removal percentages [Sutherland et al. 2004]. Using air stripping, Ramakrishnan et al. (2004) achieved more than 99% MTBE removal from distilled water at air/water ratios in the range of 105:1 to 206:1. Temperature is an important process parameter in air stripping because of the decreased MTBE volatility at lower temperatures. Also, water containing significant amounts of ferrous iron, hardness, and/or nutrients, are of concern because they can foul packed towers [Sutherland et al. 2004]. As a result, removal of MTBE by air stripping was less effective from a river water than from distilled-deionized water in one study [Wilhelm et al. 2002].

Adsorption processes have been evaluated for MTBE removal from aqueous solution and from off-gases emitted by air stripping processes. Ramakrishnan et al. (2004) compared an activated carbon and a carbonaceous resin for off-gas treatment. The MTBE adsorption capacity of the adsorbents was measured at three different relative humidities (20, 30, and 50%). While the MTBE adsorption capacity of the activated carbon was adversely affected by the presence of water vapor, that of the carbonaceous resin was similar at the different relative humidities [Ramakrishnan et al. 2004]. Testing MTBE adsorption from water, rapid

small-scale column tests (RSSCTs) with two different coal-based granular activated carbons and five different groundwaters showed that BTEX (benzene, toluene, ethylbenzene, and xylene) was preferentially adsorbed compared to MTBE [Sutherland et al. 2004], and the presence of BTEX reduced the MTBE adsorption capacity as a result. Similar results were obtained by Shih et al. (2003) with a coconut shell-based activated carbon (CC-602). The capacity reduction for MTBE due to BTX was around 30% [Shih et al. 2003]. Additionally, Shih et al. (2003) found that a higher TOC content in the water adversely affected MTBE removal because of GAC fouling associated with TOC adsorption.

Advanced oxidation processes, such as UV/$H_2O_2$ and $O_3$/$H_2O_2$ have been evaluated for MTBE removal. Results obtained by Sutherland et al. (2004) showed that only under the most efficient conditions (low alkalinity, COD, and BTEX concentrations at pH 7.0) did the electrical energy per order of magnitude removal (EE/O) values for UV/$H_2O_2$ treatment fall within typical ranges for other groundwater contaminants. These results are directly related with the ability of $H_2O_2$ to absorb the applied UV light and with •OH radical scavenging. At high COD concentrations, more •OH radical scavenging and less UV light absorption by $H_2O_2$ was observed, reducing the overall process efficiency. Also, generation of byproducts, like TBA, is a concern when considering advanced oxidation processes for MTBE removal. If these byproducts require removal, treatment costs will be higher due to the need for a higher oxidant dosage.

Comparing treatment costs for air stripping, adsorption, and advanced oxidation processes Sutherland et al. (2004) found that air stripping was the least costly treatment option for

MTBE removal at high flow rates. However, costs associated with off-gas treatment were not included in the analysis. Activated carbon adsorption was the most expensive treatment option for four of five natural waters studied. At low flow rates, the most cost-effective treatments were UV/$H_2O_2$ and $O_3$/$H_2O_2$ with the exception of the high COD water, for which the advanced oxidation processes were relatively ineffective [Sutherland et al. 2004]. However, treatment cost estimates associated with UV/$H_2O_2$ and $O_3$/$H_2O_2$ processes only considered MTBE removal and not the removal of oxidation byproducts such as TBA. Wilhelm et al. (2002) found that by using activated carbon and air stripping processes, neither of the treatments were cost-effective for removing high concentrations of MTBE in a 30 mgd water treatment plant.

## 2.3. Natural organic matter effects on organic contaminant adsorption capacity

To evaluate the adsorption capacity and effectiveness of different adsorbents for removing contaminants from aqueous solutions, adsorption isotherm experiments are performed. An isotherm relates the solid phase concentration of the contaminant to its liquid phase concentration at equilibrium. In aqueous systems, the position of the isotherm depends on adsorbent, adsorbate, and solution properties. The adsorption of organic contaminants from water results from the combination of two driving forces: the hydrophobicity of the adsorbate and the affinity of the adsorbate for the adsorbent. Hydrophobic molecules prefer to leave the aqueous phase and tend to adsorb onto a solid surface. However, hydrophilic molecules like MTBE will tend to stay in solution unless the adsorbent surface provides attractive forces that are sufficiently strong to disrupt MTBE-water bonds. Compounds such as MTBE are preferentially adsorbed in pores with a size similar to that of the adsorbate because of an increased interactions between the adsorbate and the adsorbent pore walls. The opposing pore walls in narrow pores create overlapping potential forces, which increase the adsorption forces in micropores [Pelekani and Snoeyink 1999]. In addition, the adsorption of compounds in small pores can lead to intramolecular interactions, resulting in condensation of small pockets of pure solution of the adsorbed compound [Melin 1999].

The contaminant adsorption capacity of adsorbents can be adversely affected by the presence of natural organic matter (NOM) in the water requiring treatment. The mechanisms by which NOM can compete with organic contaminants for adsorption sites are (1) pore blockage, where adsorbed NOM restricts contaminant access to pore volume and surface area, and (2)

direct competition for adsorption sites. The effect of these mechanisms on the adsorption process depends on the size of the competing NOM and the pore size distribution of the adsorbent [Pelekani and Snoeyink 1999; Kilduff et al. 1998]. When one adsorbate is a larger molecule, and a significant fraction of the adsorbent pores have sizes less than the larger adsorbate, the pore blockage mechanism is more likely to occur. On the other hand, adsorbates with similar sizes can directly compete for adsorption sites. Pelekani and Snoeyink (1999) found that pore blockage was the mechanism by which NOM competed with atrazine when an activated carbon fiber with mostly primary micropores (<8Å) and a very narrow pore size distribution was tested. Almost complete pore blockage was observed at low carbon doses. In contrast, direct competition between atrazine and NOM for adsorption sites was the competition mechanism when an activated carbon fiber with a broader pore size distribution that included both primary and secondary micropores (up to 20Å) was tested. Similar results were obtained by Li et al. (2003b) with two powdered activated carbons (PACs) with different pore size distributions.

## 2.4. MTBE adsorption on activated carbons, carbonaceous resins and high-silica zeolites

MTBE adsorption from surface and ground water has been studied fairly extensively, and a publication by the California MTBE Research Partnership has reviewed MTBE adsorption data for several activated carbons and carbonaceous resins [Melin 1999]. However, little information has been published to date on the use of high-silica zeolites for MTBE adsorption from aqueous solution. Recent work showed that high-silica zeolites may be suitable alternative adsorbents for MTBE removal from water [Li et al. 2003a; Anderson 2000]. Table 2 summarizes single-solute adsorption capacities of selected adsorbents for MTBE at equilibrium liquid phase concentrations of 100 and 1000 μg/L. MTBE adsorption capacities of high-silica zeolites exceeded those of activated carbons and carbonaceous resins by a factor of 2 to 4. Table 2 also shows that MTBE adsorption capacities of activated carbons were similar to those of carbonaceous resins.

Figure 1 compares single-solute MTBE adsorption isotherms for an all-silica Beta zeolite [Li et al. 2003a], a high-silica Mordenite zeolite [Anderson 2000], the carbonaceous resin Ambersorb 563 [Sun 1999 as reported by Melin 1999], and the activated carbon F600 [Quinlivan 2001, Li et al. 2002]. The isotherms converge at an equilibrium liquid phase concentration of about 4 μg/L, but the slopes of the MTBE isotherms on high-silica zeolites were steeper, suggesting that they are more effective for MTBE removal at higher equilibrium liquid phase concentrations.

**Table 2. Single-solute MTBE adsorption capacities at equilibrium liquid phase concentrations of 100 and 1000 µg/L for different adsorbents**

| Adsorbent | MTBE adsorption capacity (mg/g) | |
|---|---|---|
| | at $C_{eq}$ = 100 µg/L | at $C_{eq}$ = 1000 µg/L |
| Mordenite ($SiO_2/Al_2O_3$=200) | 8.0[*] | -- |
| all-silica β zeolite | 9.0[&] | -- |
| Ambersorb 563 (carbonaceous resin) | 2.0 to 4.0[+,§] | 4.0 to 18.0[+,§], 15.6[#] |
| Ambersorb 572 (carbonaceous resin) | 3.8[+] | 13.8[#] |
| CC-602 GAC (activated carbon) | 4.8[+] | 14.0[+] |
| Filtrasorb 400 | -- | 3.1[#] |

[*] Anderson (2000)
[&] Li et al. (2003)
[+] Data reported by Melin (1999)
[§] Based on the results of three studies summarized by Melin (1999)
[#] Davis and Powers (2000)

The effect of NOM on the adsorption of MTBE by the carbonaceous resin Ambersorb 572 and activated carbon GRC-22 (coconut-shell-based carbon) was evaluated by Suffet et al. (1999) [as reported by Melin 1999]. They found that the carbonaceous resin was not affected by the presence of NOM. In contrast, the MTBE adsorption capacity of the activated carbon was adversely affected by the presence of NOM.

Similar results were obtained by Hand et al. (1994) when they compared trichloroethene (TCE) adsorption capacities of the carbonaceous resin Ambersorb 563 and the activated carbon Filtrasorb 400 in organic-free water and ground water containing NOM. They found that, in the presence of NOM, the activated carbon adsorption capacity decreased by 35% relative to the single-solute adsorption capacity while the carbonaceous resin adsorption capacity was not affected after ten weeks of NOM exposure.

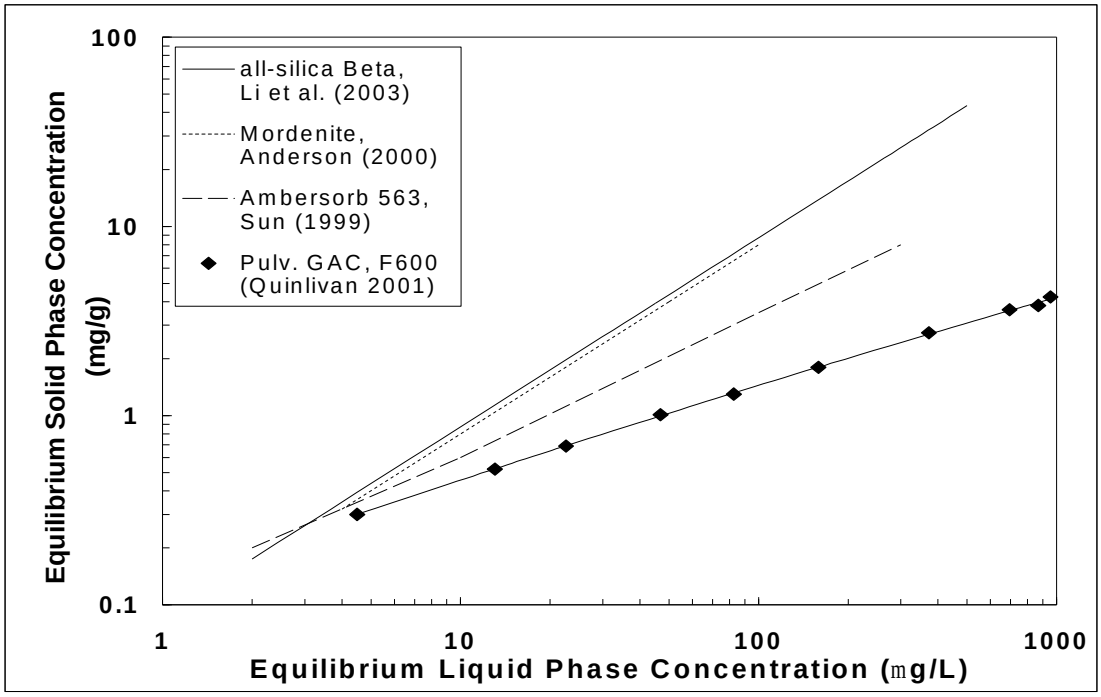


**Figure 1. Comparison of single-Solute MTBE adsorption isotherms for selected adsorbents**

## 2.5. Zeolites

The zeolite group of minerals was discovered in 1756 by the Swedish mineralogist Baron Cronstedt. It was only in the 1950s, however, when these sediments were studied in more detail by means of X-ray diffraction, that zeolites awakened the interest of professionals [Pfenninger 1998]. Today, zeolites have been turned into a high-value commercial family of materials. At this time, some 40 different natural zeolite forms are known and well characterized [Pfenninger 1998], and the number of structure types confirmed by 2001, considering natural and synthetic materials, was 133 [McCusker and Baerlocher 2001]. Zeolites are microporous materials with uniform pore dimensions, and they are attractive materials for many applications because of the following properties: they are selective adsorbents, good ion exchangers, good solid acid catalysts, and thermally stable [Pfenninger 1998, Szostak 1998]. In 1997, the total world usage of zeolites was approaching 1.6 million tons per year, the detergent industry being the biggest consumer. In the field of adsorption and desiccation, zeolites are being used for the removal of moisture and undesired substances from gas or liquid mixtures. For catalysis, zeolites are mostly used for fluid catalytic cracking applications and in the hydrocracking market [Pfenninger 1998]. Natural zeolites have been used as a soft, high-brightness additive to paper and as a selective ion exchange agent for the removal or concentration and isolation of radioactive species from waste waters generated by nuclear installations. Another application for natural zeolites is $NH_4^+$ removal in municipal wastewater treatment plants [Pfenninger 1998].

The primary zeolite building blocks are $TO_4$ tetrahedra, where T is either a $Si^{4+}$ or $Al^{3+}$ atom located at the center of the tetrahedron (Figure 2). Tetrahedra are linked via their oxygen atoms to other tetrahedra to form structural subunits, such as the sodalite unit (Figure 3), that define the framework of zeolites. Figure 3a depicts two alternative visualizations of the sodalite unit – one shows only T atoms (represented by the junctions of the schematic) while the other shows both T and O atoms. Figure 3b summarizes 8 common structural subunits. The linking of recurring structural subunits produces the crystalline framework structure of a zeolite, within which exist voids and channels of discrete and regular size. This pore size regularity makes zeolites different from other molecular sieves such as the microporous charcoal and amorphous carbon. Zeolite pore openings range from 3 to > 7 Å depending on the framework structure [Szostak 1998].

The crystalline zeolite framework carries a negative charge, and its magnitude depends on the amount of isomorphically substituted $Al^{3+}$. This charge is balanced by cations localized in non-framework positions (cavities or channels) to obtain a neutral net charge of the structure. Typical cations include the alkaline ($Li^+$, $Na^+$, $K^+$, $Rb^+$, $Cs^+$) and the alkaline earth ($Mg^{2+}$, $Ca^{2+}$, $Ba^{2+}$) cations, as well as $NH_4^+$, $H_3O^+$ ($H^+$), $TMA^+$ (tetramethylammonium) and other nitrogen-containing organic cations [Szostak 1998]. The framework charge and cations are important as they determine the ion exchange properties of zeolites. Zeolites with low $Al^{3+}$ content or constituted exclusively of $Si^{4+}$ in the tetrahedral sites have low negative or neutral framework charge and therefore exhibit a high degree of hydrophobicity and poor ion exchange capacity [Szostak 1998]. The degree of hydrophobicity, which increases with

increasing $SiO_2/Al_2O_3$ ratio of the structure, determines a zeolite's suitability for the removal of organic contaminants from aqueous solutions [Kawai et al. 1994, Li et al. 2003a].


**Figure 2. Primary building unit of zeolites [Szostak 1998].**

(a)

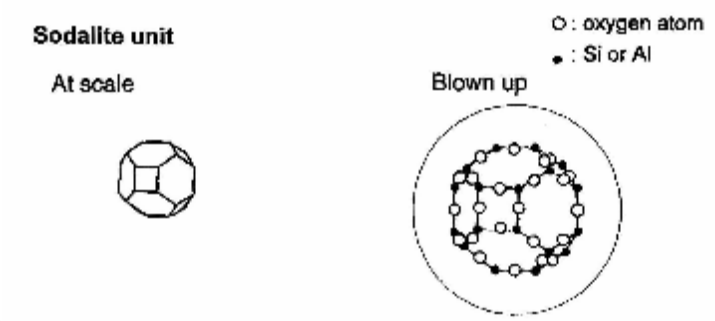


(b)

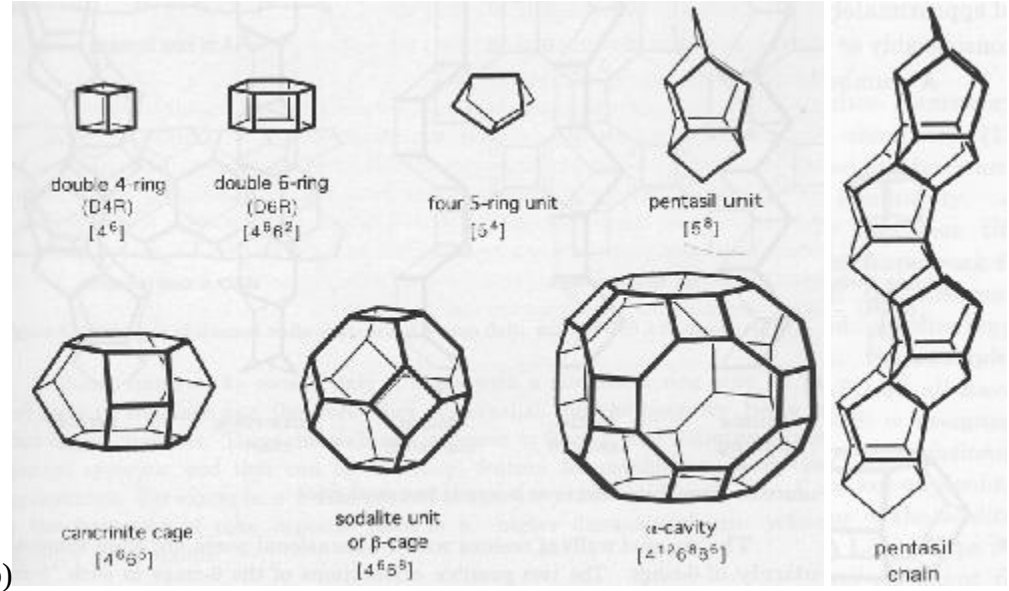


**Figure 3. Structural subunits of zeolites: (a) the sodalite cage, (b) common structural subunits [McCusker and Baerlocher 2001].**

Among the zeolites structures presently known, this work focused on four: ZSM-5/silicalite (MFI), Mordenite (MOR), Beta (*BEA), and Y (FAU) zeolites.

### *2.5.1. ZSM-5/silicalite (MFI) zeolites*

The most important member of the MFI family is the ZSM-5 zeolite. The pure silica form of ZSM-5 zeolites is known as silicalite. The 'hollow tube' representation of ZSM-5 (MFI) zeolite pores and the MFI framework are presented in Figure 4. Zeolite ZSM-5 is constructed from pentasil units that are linked together in pentasil chains (Figure 3b). Mirror images of these chains are connected by oxygen brides to form corrugated sheets with ten-ring channel openings (i.e. the perimeter of the elliptical channel opening is formed by ten T atoms). Figure 4 highlights such a corrugated sheet in the y-z plane. Oxygen bridges link each sheet to the next to form a three-dimensional structure with straight ten-ring channels parallel to the corrugations along y intersected by sinusoidal ten-ring channels perpendicular to the sheets along x (Figure 4) [McCusker and Baerlocher 2001]. The minor and major axis dimensions are 5.1 × 5.5 Å for the sinusoidal channels and 5.3 × 5.6 Å for the straight channels. The $SiO_2/Al_2O_3$ ratio of this zeolite type ranges from 20 to infinity for the pure silica form silicalite [Szostak 1992].

When adsorbed on HZSM-5 zeolites (H denoting the hydrogen cation as the exchangeable cation in the structure), linear and branched hydrocarbons behave as condensed liquids, that are capable of filling the entire pore structure [Szostak 1992]. Centi et al. (2002) found that the exchangeable cation of ZSM-5 zeolites plays a critical role in the adsorption and hydrolysis of MTBE. A hydrogen-form ZSM-5 zeolite ($SiO_2/Al_2O_3$=25) effectively

hydrolyzed MTBE to form tertiary butyl alcohol (TBA) and methanol while the sodium form of ZSM-5 with the same $SiO_2/Al_2O_3$ ratio did not react with MTBE. Centi et al. (2002) also found that a hydrogen-form ZSM-5 zeolite with a $SiO_2/Al_2O_3$ ratio of 80 had an increased catalytic activity and adsorption capacity compared with the zeolite with a $SiO_2/Al_2O_3$ ratio of 25. Water adsorption studies showed that the three-dimensional array of hydrogen-bonded water molecules cannot easily penetrate the pores of ZSM-5 zeolites without considerable distortion of the hydrogen bonds [Carrott et al. 1991], and that the quantity of adsorbed water in ZSM-5 zeolites is dependent on the zeolite hydrophobicity. As a result, silicalite exhibits a lower affinity for water than ZSM-5 zeolites with higher $Al^{3+}$ content [Kenny and Sing 1990].

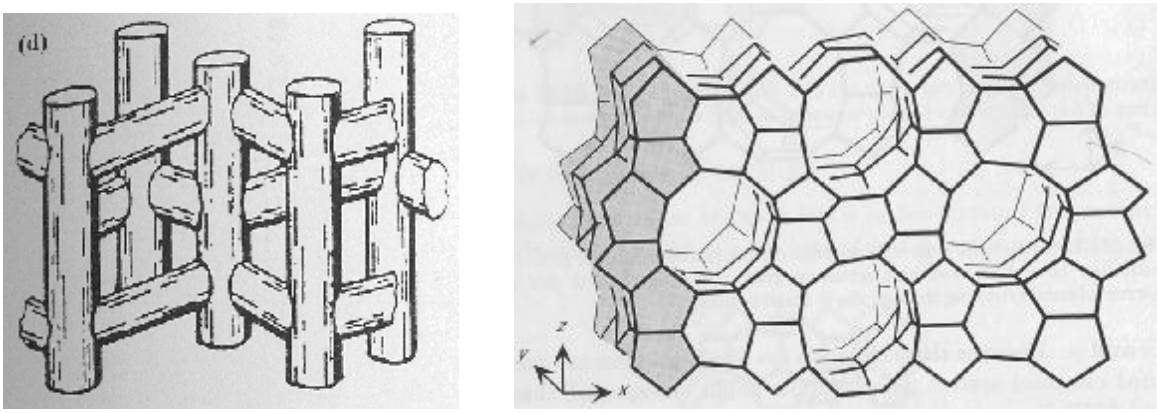


**Figure 4. The 'hollow-tube' representation of ZSM-5 zeolite pores (left) [Szostak 1998], and the MFI framework (right) [McCusker and Baerlocher 2001].**

### *2.5.2. Mordenite (MOR) zeolite*

The Mordenite framework type is formed with the "four 5-ring" subunits shown in Figure 3b. These units are linked to one another by common edges to form chains as illustrated in Figure 5, and mirror images of these chains are connected by oxygen bridges to form

corrugated sheets (highlighted in gray in Figure 5). The corrugated sheets are connected together to form oval twelve- and eight-ring channels along the z direction (Figure 5). These channels are connected by eight-ring channels that are displaced with respect to one another (Figure 5). The twelve- and eight-ring channels have dimensions of $6.5 \times 7.0$ Å and $2.6 \times 5.7$ Å, respectively. Given the small size of the eight-ring channels, the MOR channel system is effectively one-dimensional instead of two-dimensional [McCusker and Baerlocher 2001]. Mordenite is highly selective for cesium and strontium, making it suitable for the treatment of radioactive waste [Szostak 1992].

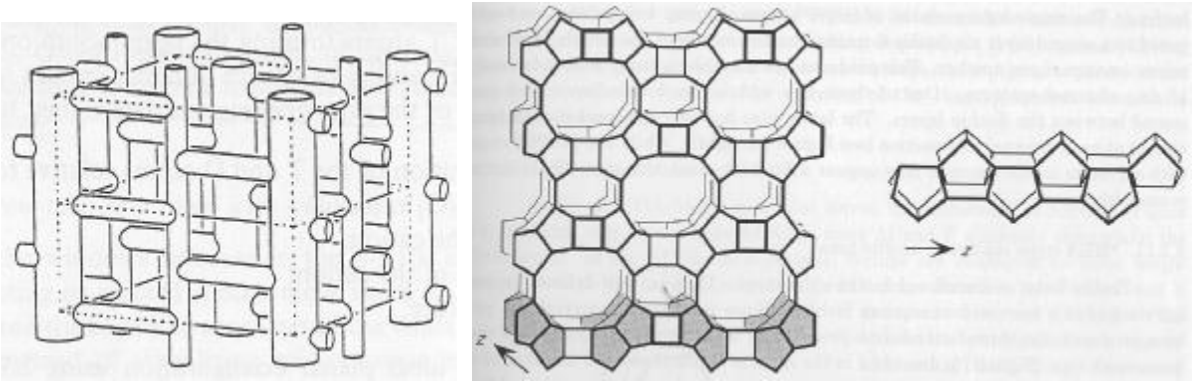

**Figure 5. Hollow-tube representation of Mordenite (MOR) zeolite pores (left) [Szostak 1998], and the MOR framework (right) [McCusker and Baerlocher 2001].**

### *2.5.3. Beta (*BEA) zeolite*

Beta zeolites have well-defined layers (comprised of "four 5-ring" subunits (Figure 3b) joined by 4-ring subunits) that are stacked in a disordered way along the z direction. No ordered material has been produced to date. The asterisk preceding the three-letter code for this zeolite type denotes that the framework type in Figure 6 is an idealized end member of a series. Adjacent layers, shown separately in Figure 6, are connected by a rotation of 90°. The rotation can be in a clockwise or counterclockwise direction, generating the disorder of the

framework. Despite this disorder, a three-dimensional twelve-ring channel system is formed [McCusker and Baerlocher 2001]. The pore dimensions of the channel system are $6.5 \times 5.6$ Å and $7.5 \times 5.7$ Å [Szostak 1992].

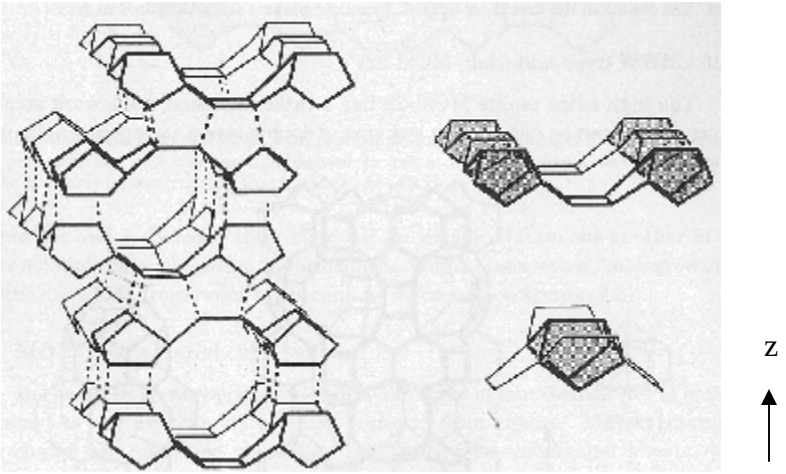


**Figure 6. The idealized *BEA framework type with all layers related to one another via counterclockwise rotation. The well-defined layer, and its building unit are shown separately [McCusker and Baerlocher 2001].**

### *2.5.4. Y (FAU) zeolite*

The framework of the faujasite structure can be described as a linkage of $TO_4$ tetrahedra in a truncated octahedron. The truncated octahedron is referred to as the sodalite unit or sodalite cage (Figure 3) [Szostak 1992]. In the faujasite structure, the sodalite units are linked together at the six-ring ends (i.e., the hexagonal faces of the sodalite unit) in a manner that is analogous to the arrangement of C-atoms in diamonds (Figure 7). The Y-zeolite (faujasite structure) has circular, 12-ring windows with a diameter of 7.4 Å (or $7.4 \times 7.4$ Å) and supercages with a diameter of about 13 Å [Rouquerol et al. 1999].

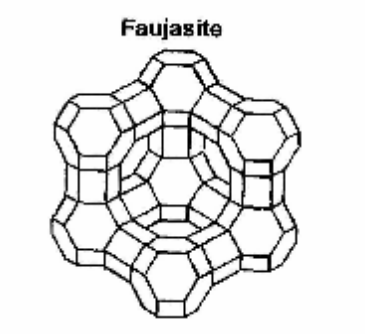


**Figure 7.The faujasite framework type (zeolites X and Y) [Rouquerol et al. 1999].**

# 3. MATERIALS AND METHODS

## 3.1. Materials

### *3.1.1. Water*

Isotherm experiments were conducted in ultrapure laboratory water (Raleigh, NC, tap water treated by reverse osmosis, ion exchange, and granular activated carbon adsorption, resistance ≥ 14.85 MΩ/cm). Ultrapure water was amended with a 1 mM phosphate buffer (0.5 mM $Na_2HPO_4 \bullet 2H_2O$ and 0.5 mM $NaH_2PO_4 \bullet 7H_2O$) to maintain a pH of 7.2.

The effect of NOM on MTBE adsorption capacity was evaluated with raw Tar River water (TRW) that was collected by the Greenville Utilities Commission (Greenville, NC). Prior to use in isotherm experiments, the water was vacuum-filtered through a 0.45-µm nylon membrane filter (Magna-R, MSI, Westboro, MA) that was placed in a 47-mm glass microanalysis filter holder (Fisher Scientific, Pittsburgh, PA). The TOC of filtered TRW was 6.1 mg/L, the pH was 7.8, and the total alkalinity was 25 mg/L as $CaCO_3$.

### *3.1.2. Adsorbents*

Ten commercially available zeolite samples were obtained as summarized in Table 3. In addition, commercially available granular activated carbons (GACs) were obtained from Calgon Carbon Corporation (coal-based F-600) and US Filter (coconut-shell-based CC-602

and coal-based UC-830), and a carbonaceous resin was obtained from Supelco (Ambersorb 563). To enhance adsorption rates, all pelletized zeolites, the GACs, and the Ambersorb 563 resin were pulverized with a mortar and pestle until >95% by mass passed a 74-µm sieve (200 U.S. mesh). Upon sieving, the portion remaining on the sieve was recombined with the portion that passed through the sieve to prevent bias as a result of any physical and/or chemical differences between the two fractions. The pulverized adsorbent was dried at 105°C for one day and stored in a desiccator.

**Table 3. Zeolite characteristics**

| Zeolite type | Manufacturer's ID code | Manufacturer | Cation [(a)] | Pore dimensions [(a)] | $SiO_2/Al_2O_3$ [(a)] | BET surface area ($m^2/g$) |
|---|---|---|---|---|---|---|
| ZSM-5 | H-MFI-90 | Süd-Chemie, Munich, Germany | $H^+$ | 0.53 nm*0.55 nm (10-ring) | 90 | 322 |
| ZSM-5 | H-MFI-240 | Süd-Chemie, Munich, Germany | $H^+$ | 0.53 nm*0.55 nm (10-ring) | 240 | 313 |
| ZSM-5 | CBV-28014 | Zeolyst International, Valley Forge, PA | $NH_4^+$ | 0.53 nm*0.55 nm (10-ring) | 280 | 345 |
| ZSM-5 | SN-300 | ALSI-PENTA GmbH, Schwandorf, Germany | $Na^+$ | 0.53 nm*0.55 nm (10-ring) | 300 | 356 |
| ZSM-5 | H-MFI-400 | Süd-Chemie, Munich, Germany | $H^+$ | 0.53 nm*0.55 nm (10-ring) | 400 | 304 |
| Silicalite | HiSiv 3000 | UOP, Mount Laurel, NJ | | 0.53 nm*0.55 nm (10-ring) | 700 | 282 |
| Mordenite | HSZ-690HOA | Tosoh Corporation, Tokyo, Japan | $H^+$ | 0.65 nm*0.70 nm (12-ring) | 230 | 505 |
| Beta | CP811C-300 | Zeolyst International, Valley Forge, PA | $H^+$ | 0.76 nm*0.64 nm (12-ring) | 300 | 544 |
| Y | HiSiv 1000 | UOP, Mount Laurel, NJ | | 0.74 nm*0.74 nm (12-ring) | 12 | 550 |
| Y | HSZ-390HUA | Tosoh Corporation, Tokyo, Japan | $H^+$ | 0.74 nm*0.74 nm (12-ring) | 810 | 806 |

[(a)] Based on data provided by each manufacturer

### *3.1.3. Adsorbate*

MTBE was the targeted micropollutant for this study. Because of its ether oxygen, MTBE is relatively hydrophilic (aqueous solubility at 25°C ≈ 51,000 mg/L, log $K_{ow}$ = 1.24). For single-solute isotherms, MTBE stock solutions were prepared in ultrapure water at a concentration of approximately 2,700 mg/L. For isotherm experiments conducted in the presence of competing and preloaded NOM, MTBE stock solutions were prepared in ultrapure water at a concentration of approximately 270 mg/L.

## 3.2. Methods

### *3.2.1. Adsorbent characterization*

BET surface areas were determined from $N_2$ isotherm data collected at 77 K (Autosorb-1-MP, Quantachrome Corporation, Boynton Beach, FL). Prior to analysis, adsorbent samples were outgassed for 20 hours at 423 K. BET surface areas were determined from 18-point adsorption isotherms that were completed with a 0.2-g sample in the 0.01-0.3 relative pressure range.

### *3.2.2. Isotherm experiments*

Adsorption isotherm experiments were performed using adsorbent doses between 10 and 3,000 mg/L. Depending on the targeted adsorbent dose, adsorbents were transferred into 4-oz., 8-oz., or 16-oz. amber glass bottles. After filling the isotherm bottles with amended ultrapure water or TRW, MTBE stock solution was added with a constant rate syringe (CR-700-200, Hamilton Co., Reno, NV) to yield an initial concentration of about 1000 µg/L (single-solute isotherms) or about 100 µg/L (isotherms in the presence of co-adsorbing NOM). Some single-solute isotherm experiments were also conducted with an initial concentration of 100 µg/L to obtain equilibrium liquid phase concentrations that were in a range similar to that obtained in isotherm experiments employing TRW. Once MTBE was added to a bottle, it was topped off immediately with amended ultrapure water or TRW to create headspace-free conditions and capped using PTFE-faced silicon septa and open-top

closures. A mixing time of 3 weeks in a rotary tumbler was sufficient to reach adsorption equilibrium, as established in screening tests. For experiments evaluating the effects of preloaded NOM, adsorbent-containing isotherm bottles were filled to the top with TRW and tumbled for 3 to 4 weeks prior to MTBE addition. After the preloading period, MTBE was spiked as above to yield an initial concentration of about 100 µg/L. Following MTBE addition, the samples were mixed for 3 additional weeks before analysis. MTBE losses were not observed in triplicate blanks containing no adsorbent over that time period. Upon equilibration, samples were filtered through 0.22-µm MAGNA nylon membrane filters (Osmonics/MSI, Westboro, MA) that were placed in a 25-mm stainless steel syringe filter holder (Fisher, Pittsburgh, PA). The filters were soaked overnight in organic-free water prior to use.

### *3.2.3. MTBE analysis*

Aqueous samples were analyzed for MTBE using a purge and trap concentrator (Tekmar 3100, Cincinnati, OH) that was connected to a gas chromatograph (Shimadzu 14a, Columbia, MD) equipped with a 30-m column (J&W Scientific DB-VRX, I.D. 0.45 mm, liner thickness 2.55 µm, Folsom, CA) and a flame ionization detector (FID). Samples (5 mL) were purged with nitrogen gas at 36°C for 12 min. The analytes were trapped on a Vocarb 3000 trap (Supelco, Bellefonte, PA) and desorbed for 2 min at 255°C. The GC oven temperature was maintained at 40°C for 3 min, was increased at 20°C/min and held at 90°C for 2.5 minutes, increased at 20°C/min and held at 140°C for 1 minute, and finally increased at 40°C/min and held at 240°C for 1 min. MTBE concentrations were quantified using external standards.

### 3.3. Adsorption isotherm data modeling

Adsorption isotherm data obtained with activated carbon are frequently described with the Freundlich isotherm equation ($q_e = K \cdot C_e^{1/n}$, where $q_e$ and $C_e$ are the solid phase and liquid phase equilibrium MTBE concentrations, respectively, and K and 1/n are the Freundlich isotherm parameters). This equation yields a straight line in a double-logarithmic plot. However, the MTBE adsorption data for zeolites and the carbonaceous resins could not be described adequately using the Freundlich equation because they began to plateau at high equilibrium liquid phase MTBE concentrations. Parker (1995) showed that the Dubinin-Astakhov (DA) isotherm equation was the most suitable equation, among fifteen studied, for the representation of trichloroethene (TCE) adsorption on carbonaceous resins. Also, Davis and Powers (2000) determined that the DA model was well suited for describing MTBE adsorption isotherm data for two carbonaceous resins. Recently, Kilduff and Karanfil (2002) also used the DA model to evaluate the effects of preloaded NOM on TCE adsorption by GAC. The DA isotherm model is based on Dubinin's theory of micropore volume filling and has the form shown in equation 1 (Parker 1995):

$$q_e = q_m \cdot \exp\left[-\left(\frac{A}{E}\right)^n\right] \qquad \text{(eq. 1)}$$

where A is the adsorption potential (J/mol):

$$A = RT \cdot \ln\left(\frac{C_{sat}}{C_e}\right) \qquad \text{(eq. 2)}$$

$q_m$, n, E are the three adjustable parameters of the DA isotherm model, R is the ideal gas constant (8.314 J $mol^{-1}$ $K^{-1}$), T is the absolute temperature (K), and $C_{sat}$ is the aqueous solubility of MTBE (51,000 mg/L). The adjustable parameters of the model represent physical characteristics of the adsorbate and adsorbent (Parker 1995). The maximum adsorption capacity, $q_m$, represents the filling of adsorbent micropores. E is the adsorption potential at which the capacity is 36.8% of the maximum capacity. The parameter n represents the heterogeneity of the adsorbent pores and describes the curvature of the isotherm.

DA parameters were determined with the procedure NLIN (fitting of nonlinear equations) in SAS version 8.2 using the natural-log transform of equation 1. The objective function used to calculate the residual sum of squares was:

$$Objective\ \ function = \min \sum_{i=1}^{n} \left[ \ln\left(q_{e,meas}\right)_i - \ln\left(q_{e,calc}\right)_i \right]^2 \qquad \text{(eq. 3)}$$

where $q_{e,meas}$ and $q_{e,calc}$ are the measured and model-predicted equilibrium solid phase MTBE concentrations for data point i, respectively, and n is ther number of isotherm data points.

The goodness of fit was quantified by the coefficient of determination ($R^2$) as defined in equation 4 [Draper and Smith 1981]:

$$R^2 = 1 - \frac{RSS_p}{CTSS} \qquad \text{(eq. 4)}$$

where $RSS_p$ is the residual sum of squares, and CTSS is the corrected total sum of squares as reported by the SAS software.

## 4. RESULTS AND DISCUSSION

### 4.1. Adsorbent properties

Ten commercially available zeolites were tested, and their properties are summarized in Table 3. The selected zeolites differed in both pore dimensions and hydrophobicity. The zeolite hydrophobicity is expressed by the $SiO_2/Al_2O_3$ ratio, where a higher ratio value indicates a zeolite with a more hydrophobic surface. In contrast to activated carbons that exhibit relatively broad pore size distributions, zeolites are microporous molecular sieves with well-defined pore sizes. Of the selected zeolites, the silicalite and ZSM-5 varieties exhibit the smallest pores (~5.5 Å diameter) while the Y varieties exhibit the largest pores (7.4 Å diameter). It should be noted that ZSM-5 and silicalite are structurally identical; silicalite is essentially an all-silica adsorbent while ZSM-5 has a higher $Al_2O_3$ content. To assess effects of zeolite hydrophobicity on MTBE adsorption, $SiO_2/Al_2O_3$ ratios from 90 to 700 were evaluated for the ZSM-5/silicalite zeolite category. To assess pore structure effects on MTBE adsorption, ZSM-5, Mordenite, and Beta pore structures were evaluated at $SiO_2/Al_2O_3$ ratios in the 200 to 300 range. To assess the effect of exchangeable cations on MTBE adsorption, ZSM-5 zeolites in the $H^+$ form, $NH_4^+$ form, and $Na^+$ form were tested at similar $SiO_2/Al_2O_3$ ratios (240-300).

BET surface areas of the zeolites ranged from about 280 to 800 $m^2/g$ and were lower than those measured for activated carbons. The BET surface areas of the activated carbons evaluated in this study were 820 $m^2/g$ for F600 GAC, 990 $m^2/g$ for UC-830 GAC, and 1140

$m^2/g$ for CC-602 GAC. The BET surface area obtained for the carbonaceous resin Ambersorb 563 was 515 $m^2/g$. BET surface areas of the Süd-Chemie zeolites decreased slightly as the $SiO_2/Al_2O_3$ ratio increased from 90 to 400 (Table 3). This result is consistent with prior studies, in which a given zeolite product was dealuminated [Kawai et al. 1994, Li et al. 2003]. The decrease in BET surface area upon dealumination results from structural degradation (partial destruction of the zeolite framework) and the concomitant formation of amorphous material.

### 4.2. Single-solute MTBE isotherms

Single-solute MTBE adsorption isotherm experiments were conducted in ultrapure water buffered with 1 mM phosphate buffer at pH 7.2. Figure 8 compares single-solute MTBE isotherm data for different zeolite pore structures ($SiO_2/Al_2O_3$ ratio range: 230-300), a carbonaceous resin, and three pulverized GACs. Figure 8 illustrates that the carbonaceous resin (Ambersorb 563) exhibited the largest MTBE adsorption capacity when the equilibrium liquid-phase MTBE concentration was less than about 30 µg/L. In contrast, the ZSM-5 zeolite (CBV-28014) exhibited the largest MTBE adsorption capacity at higher liquid-phase MTBE concentrations. The mordenite zeolite isotherm followed the ZSM-5 zeolite isotherm at low concentrations and the carbonaceous resin isotherm at higher liquid-phase concentrations. Compared to the carbonaceous resin, the ZSM-5 zeolites, and the mordenite zeolite, the MTBE adsorption capacity of the pulverized GACs was considerably smaller (Figure 8). The beta zeolite (CP811C-300) was not effective for MTBE adsorption from

aqueous solution (Figure 8), and MTBE adsorption was negligible on the Y-zeolites (data not shown).

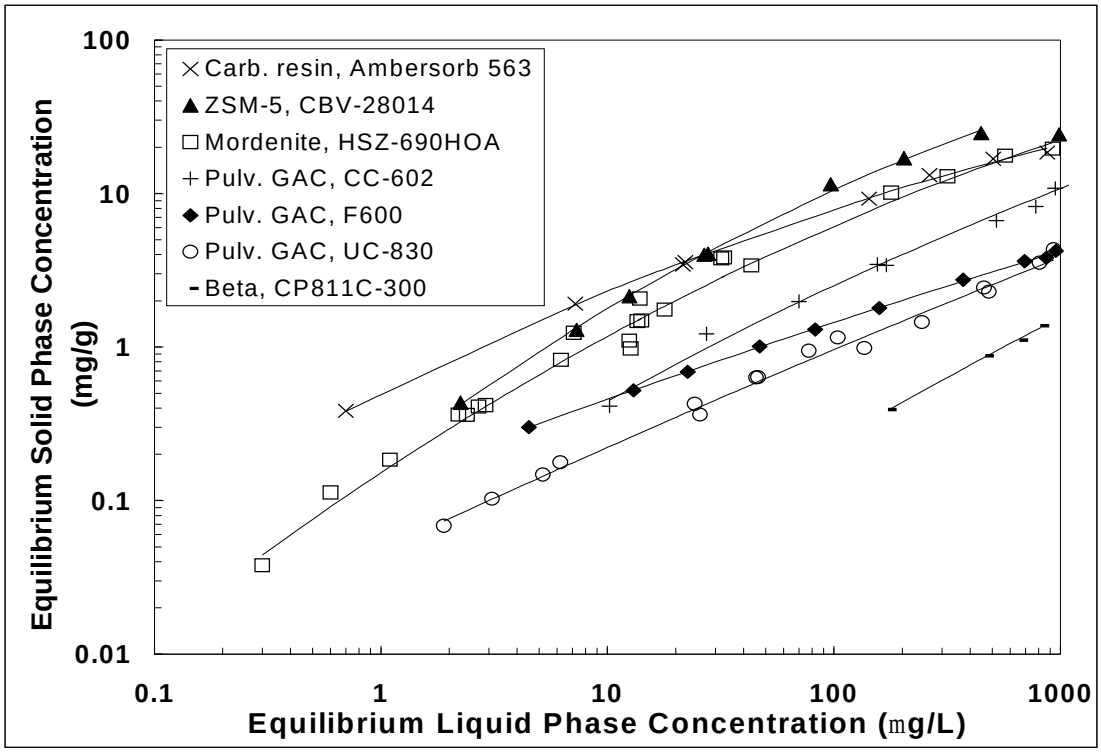


**Figure 8. Comparison of single-solute MTBE adsorption isotherms for different adsorbents. Lines represent Dubinin-Astakhov isotherm model fits.**

The isotherms shown in Figure 8 have shallower slopes than those obtained by Anderson (2000) and Li et al. (2003a). As a result, the MTBE adsorption capacities of the high-silica zeolites studied by Anderson (2000) and Li et al. (2003a) were higher than that of the carbonaceous resin at high equilibrium liquid-phase concentrations but similar to that of the F600 GAC at equilibrium liquid-phase concentrations below about 5 µg/L. However, MTBE-zeolite contact times in the previous studies were only 15 minutes [Anderson 2000] or 30 minutes [Li et al. 2003a] before liquid-phase MTBE concentrations were analyzed. These

contact times were probably too short to reach adsorption equilibrium. As a result, the MTBE liquid-phase concentrations were higher than what they would be at equilibrium, especially at high adsorbent doses, making the isotherm slopes of Anderson (2000) and Li et al. (2003a) steeper than those obtained in the current study.

The negligible adsorption capacity of the Y zeolites was unexpected because the pore openings of Y zeolites are only about 2 Å larger than those of the silicalite/ZSM-5 zeolites. However, recent studies have suggested that the larger pore size of hydrophobic Y zeolites is sufficient to permit pore filling with a continuous liquid-like water phase [Giaya and Thompson 2002]. As a result, a hydrophobic Y zeolite adsorbed TCE only poorly from aqueous solution [Giaya et al. 2000]. However, it is unclear why the hydrophobic Y zeolite performed so much more poorly than an activated carbon given that the presence of a continuous liquid-like water phase can be expected in the pores of both adsorbents [Giaya et al. 2000].

As shown in Table 3, ZSM-5/silicalite zeolites with a wide range of $SiO_2/Al_2O_3$ ratios (90-700) and with different exchangeable cations ($H^+$, $Na^+$, $NH_4^+$) were tested. Based on prior studies reported in the literature [Kawai et al. 1994; Centi et al. 2002; Centi and Perathoner 2003; Li et al. 2003a], it was hypothesized that the MTBE adsorption capacity of ZSM-5 zeolites would increase with increasing $SiO_2/Al_2O_3$ ratio. Furthermore, by testing a range of exchangeable cations, it was possible to confirm whether ZSM-5 zeolites in the $H^+$ form catalyzed MTBE hydrolysis [Centi et al. 2002] at the conditions tested in the current study. Figure 9 compares BET-surface-area-normalized MTBE adsorption capacities for six

silicalite/ZSM-5 zeolites with different hydrophobicities and exchangeable cations, and Figure 10 shows the BET-surface-area-normalized MTBE adsorption capacities for the six silicalite/ZSM-5 zeolites at an equilibrium liquid phase concentration of 10 µg/L as a function of the zeolite $SiO_2/Al_2O_3$ ratio.

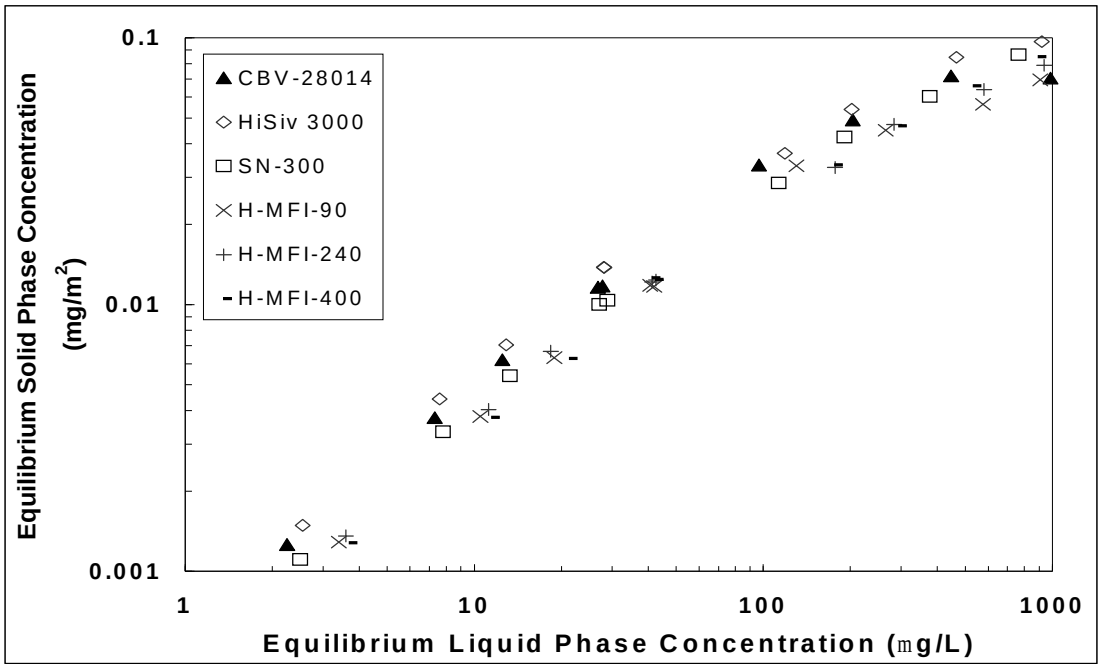


**Figure 9. Comparison of single-solute MTBE adsorption isotherms for different silicalite/ZSM-5 zeolites. Equilibrium solid phase concentrations were normalized by the BET surface area.**

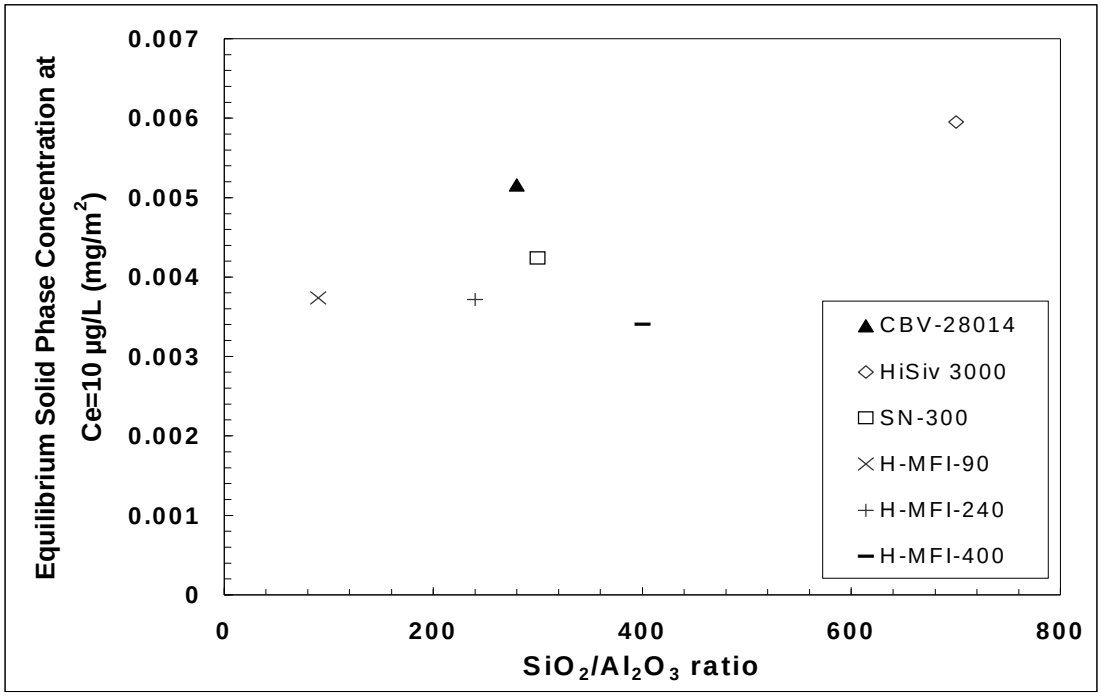


**Figure 10. Effect of zeolite $SiO_2/Al_2O_3$ ratio on MTBE adsorption capacity. Equilibrium solid phase concentrations at $C_e$ = 10 µg/L were calculated with the Dubinin-Astakhov equation using the parameters shown in Table 4 and normalized by the BET surface area.**

Differences among the MTBE isotherms depicted in Figure 9 were small, and Figure 10 suggests that no consistent trend exists between the MTBE adsorption capacity and the $SiO_2/Al_2O_3$ ratio of the tested silicalite/ZSM-5. This result was somewhat surprising in light of results of prior studies [Kawai et al. 1994; Centi et al. 2002; Centi and Perathoner 2003; Li et al. 2003a]. However, Centi et al. (2002) tested ZSM-5 zeolites ($SiO_2/Al_2O_3$ ratios of 25 and 80) that were less hydrophobic than those evaluated in this study. Kawai et al. (1994) studied a broader hydrophobicity range for both ZSM-5 and Y zeolites ($SiO_2/Al_2O_3$ ratios of ZSM-5 zeolites ranged from 25 to 1000 and from 5.5 to 770 for Y zeolites). For ZSM-5 zeolites they obtained a large difference in chloroform adsorption capacity between $SiO_2/Al_2O_3$ ratios of 25 and 70, but only small differences between $SiO_2/Al_2O_3$ ratios of 70 and 1000. For Y zeolites substantial differences in adsorption capacity were observed

between $SiO_2/Al_2O_3$ ratios of 5.5 and 224, but above this value, only small differences were obtained. These results suggest that $SiO_2/Al_2O_3$ ratios in excess of about 100 may only have a small effect on organic contaminant adsorption from the aqueous phase.

Adsorption of organic contaminants from water is energetically favored on activated carbons with hydrophobic pore surfaces because the target adsorbate is able to displace the continuous liquid-like water phase in hydrophobic activated carbon pores more easily [e.g. Li et al. 2002]. However, it appears that the pores of silicalite/ZSM-5 are so small that they disrupt hydrogen bonds of water to the extent that a continuous liquid water phase is not present in silicalite/ZSM-5 pores [Carrott et al. 1991; Giaya and Thompson 2002]. The absence of a continuous liquid water phase in the silicalite/ZSM-5 pores may therefore explain why the $SiO_2/Al_2O_3$ ratio had only a small effect on MTBE adsorption over the $SiO_2/Al_2O_3$ range evaluated in this study.

The results depicted in Figure 9 also suggest that the exchangeable cation of the zeolites had no clear effect on MTBE removal. Both the $Na^+$ form (SN-300) and the $NH_4^+$ form (CBV-28014) of the ZSM-5 zeolites exhibited MTBE adsorption capacities that matched (or exceeded) those of the ZSM-5 zeolites in the $H^+$ form (H-MFI series). This result differs from that of Centi et al. (2002) who suggested that the $H^+$ form of ZSM-5 zeolites catalyzes the hydrolysis of MTBE while the $Na^+$ form of ZSM-5 zeolites does not. MTBE hydrolysis would lead to the formation of tertiary-butyl alcohol (TBA) and methanol, and the appearance of these products was measured by Centi et al. (2002) in tests, in which solutions containing relatively high MTBE concentrations (2000-4000 mg/L) were contacted with

large doses of ZSM-5 zeolites in the $H^+$ form (~10 g/L). The similarity of the MTBE isotherms for ZSM-5 zeolites in the $H^+$ and $Na^+$ forms in Figure 9 and the absence of TBA in the zeolite-equilibrated solutions suggests that the MTBE removal mechanism was similar for both the $H^+$ and $Na^+$ forms and that catalytic hydrolysis in the presence of the $H^+$ form may therefore be negligible at the conditions tested in this study. Also, the zeolite $SiO_2/Al_2O_3$ ratios evaluated in the current study were higher than those tested by Centi et al. (2002). The absence of MTBE hydrolysis in the current study was considered to be a positive result because the hydrolysis product TBA may pose greater health risks and removal challenges than MTBE.

In this work sodium cations were present in solution at a concentration of 1.5 mM in all single-solute tests because of the salts used for the buffer preparation. This $Na^+$ concentration is fairly typical of that encountered in many natural waters [Stumm and Morgan 1996]. It may be possible that the $Na^+$ ions of the buffer replaced exchangeable $H^+$ or $NH_4^+$ ions when $H^+$ or $NH_4^+$ forms of the ZSM-5 zeolites were tested. As a result, all zeolites may have been in the sodium form during the adsorption experiments, in which case no catalytic hydrolysis should have occurred during the experiments. To evaluate whether the buffer affected MTBE removal by zeolites, isotherm experiments without buffer addition were conducted with several silicalite/ZSM-5 zeolites and compared to isotherm data collected in the presence of the buffer [CBV-28014, $NH_4^+$ form (Figure 11), SN-300, $Na^+$ form (Figure 12), H-MFI-240, $H^+$ form (Figure 13), HiSiv 3000, pure silica form/silicalite (Figure 14)]. The results in Figures 11-14 further suggest that the presence of neither sodium and nor phosphate species affected MTBE adsorption/removal at the tested MTBE concentrations and adsorbent doses.

### 4.3. MTBE isotherms in the presence of co-adsorbing and preloaded NOM

MTBE isotherm experiments in the presence of competing and preloaded NOM were conducted in filtered Tar River water (TRW). Figures 11 to 14 compare single-solute MTBE isotherm data with MTBE isotherm data obtained in the presence of co-adsorbing and preloaded NOM for silicalite/ZSM-5 zeolites [CBV-28014, $NH_4^+$ form (Figure 11), SN-300, $Na^+$ form (Figure 12), H-MFI-240, $H^+$ form (Figure 13), HiSiv 3000, pure silica form/silicalite (Figure 14)], and the results suggest that NOM had either a negligible or a small effect on MTBE adsorption capacity. With the sodium-form ZSM-5 zeolite (SN-300), a decrease in MTBE adsorption capacity was apparent at the lowest measured MTBE concentrations following NOM preloading (Figure 12). However, this observation is most likely due to uncertainties in quantifying MTBE concentrations below 1 µg/L. For the silicalite zeolite (HiSiv 3000, Figure 14), the decrease in MTBE adsorption capacity at low adsorbent doses in the presence of co-adsorbing and preloaded NOM may be a result of pore blockage by NOM molecules that adsorbed at the entrances of zeolites pores.

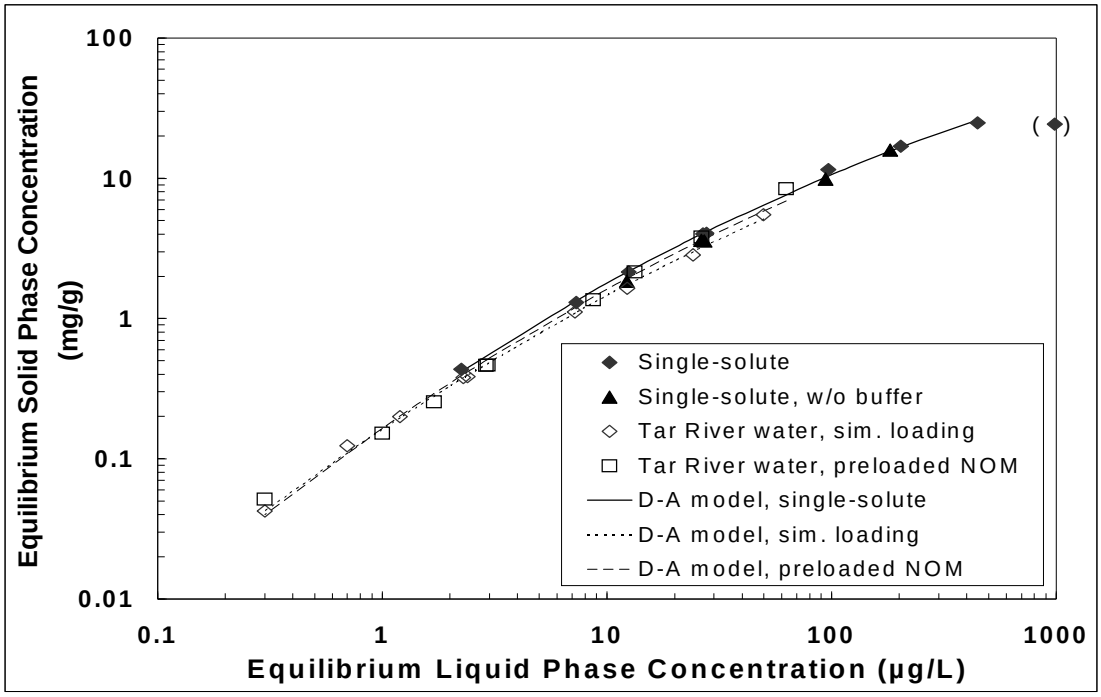


**Figure 11. Comparison of MTBE adsorption isotherms in ultrapure and Tar River water on ZSM-5 zeolite CBV-28014 ($NH_4^+$ form). Lines represent Dubinin-Astakhov isotherm model fits. Data point in parentheses was not included in DA parameter estimation.**

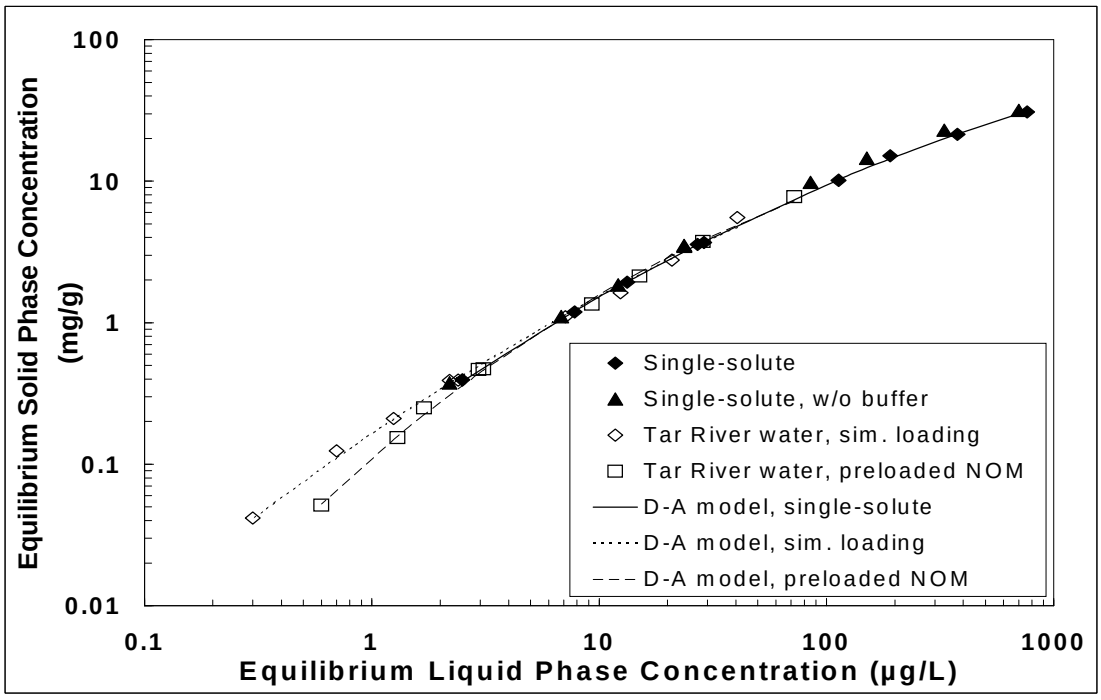


**Figure 12. Comparison of MTBE adsorption isotherms in ultrapure and Tar River water on ZSM-5 zeolite SN-300 ($Na^+$ form). Lines represent Dubinin-Astakhov isotherm model fits.**

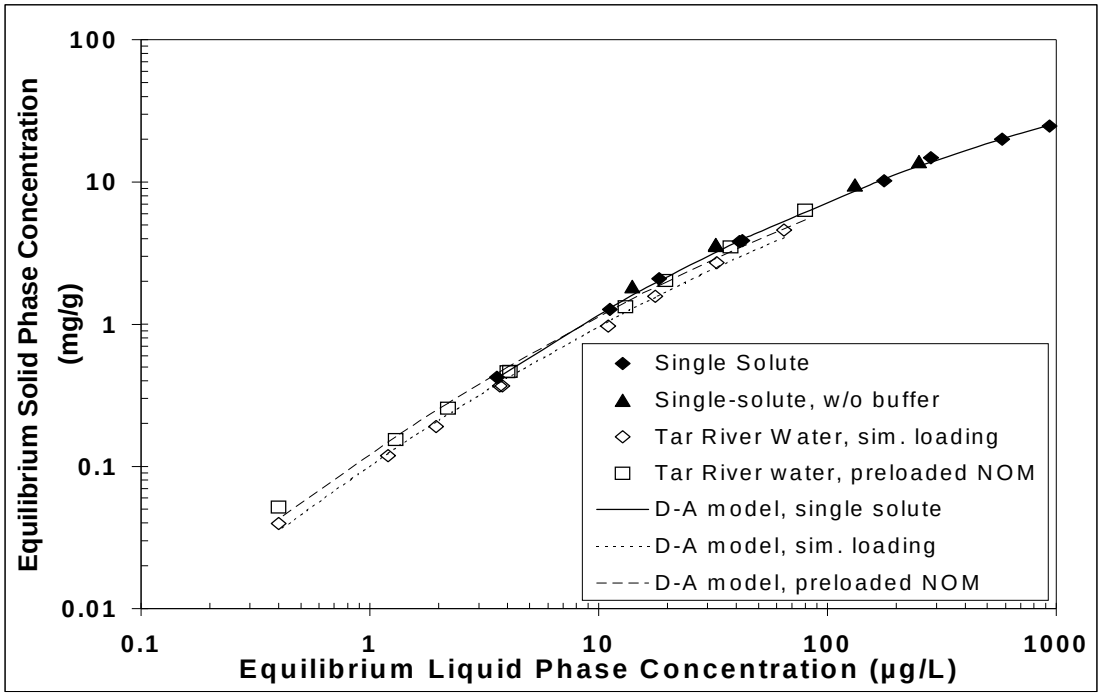


**Figure 13. Comparison of MTBE adsorption isotherms in ultrapure and Tar River water on ZSM-5 zeolite H-MFI-240 ($H^+$ form). Lines represent Dubinin-Astakhov isotherm model fits.**

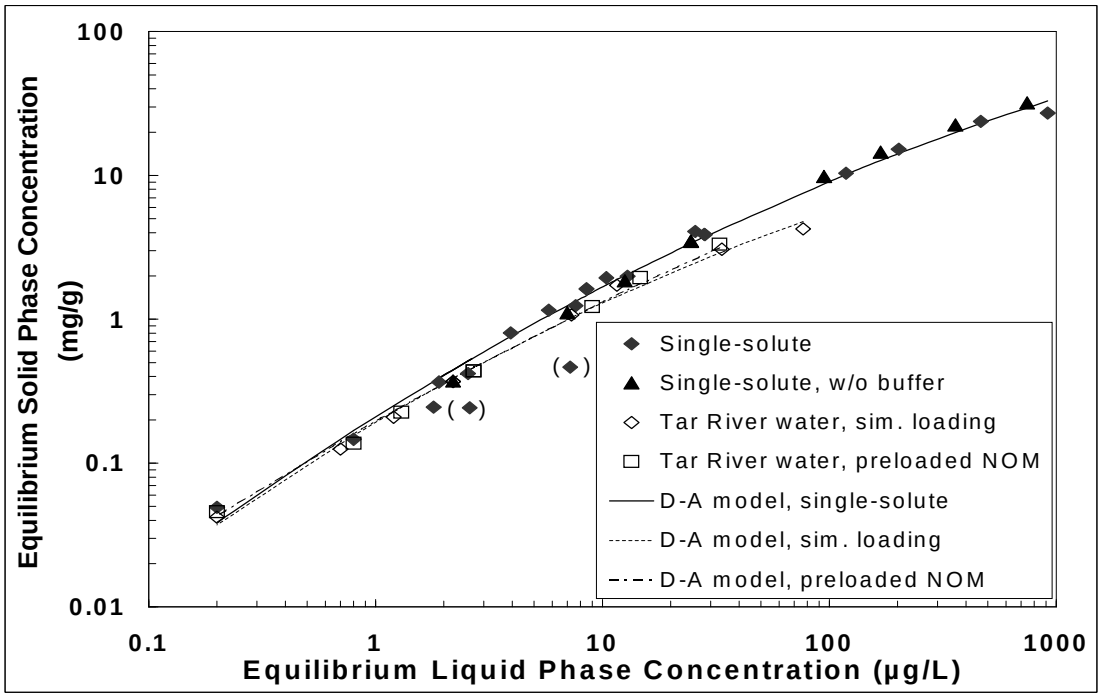


**Figure 14. Comparison of MTBE adsorption isotherms in ultrapure and Tar River water on silicalite zeolite HiSiv 3000. Lines represent Dubinin-Astakhov isotherm model fits. Data points in parentheses were not included in DA parameter estimation.**

For the mordenite zeolite, Figure 15 shows that the single-solute adsorption isotherm obtained at an initial MTBE concentration of 1000 µg/L (equilibrium liquid-phase MTBE concentrations in the range of 3 to 925 µg/L) exhibited a continuous increase in adsorption capacity as the liquid phase concentration increased. However, the single-solute adsorption isotherm obtained with a lower initial MTBE concentration of 100 µg/L (equilibrium liquid-phase MTBE concentrations in the range of 0.3 to 108 µg/L) exhibited the same trend that was obtained with preloaded NOM; i.e. it deviated from the single-solute isotherm obtained with the higher initial MTBE concentration at low adsorbent doses. As a result, it is not clear to what extent the MTBE adsorption capacity of the mordenite zeolite was affected by the presence of NOM.

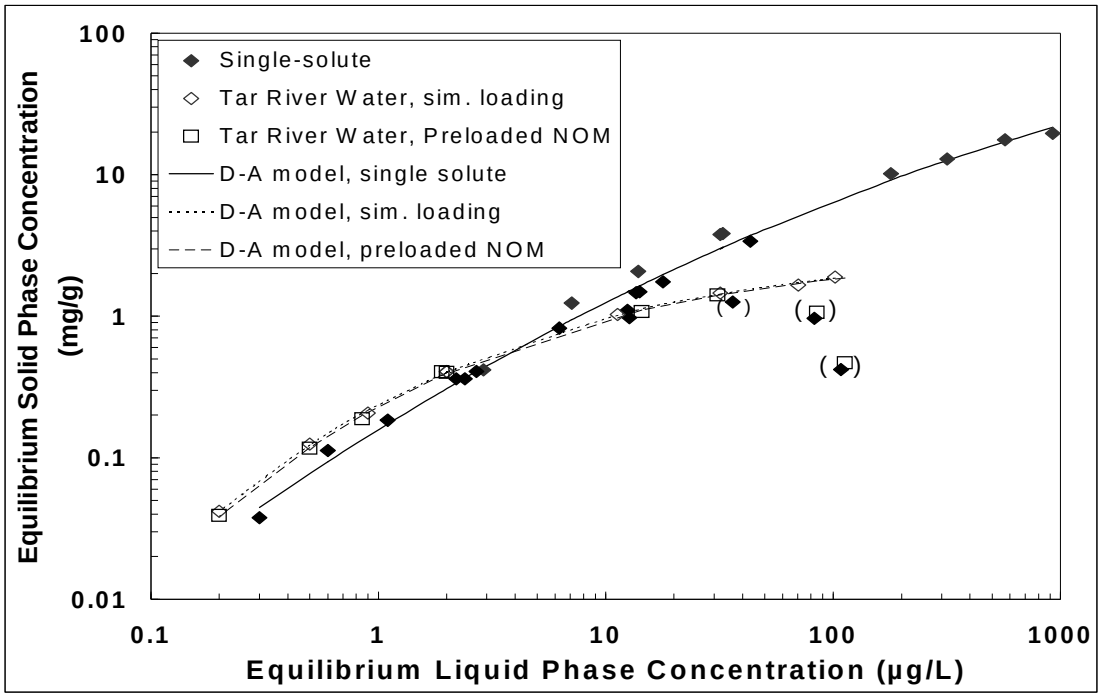


**Figure 15. Comparison of MTBE adsorption isotherms in ultrapure and Tar River water on Mordenite zeolite HSZ-690HOA. Lines represent Dubinin-Astakhov isotherm model fits. Data points in parentheses were not included in DA parameter estimation.**

Figure 16 compares MTBE adsorption capacities of the carbonaceous resin Ambersorb 563 in ultrapure water and in the presence of co-adsorbing and preloaded NOM. The MTBE isotherm data obtained for the Ambersorb 563 carbonaceous resin show that both co-adsorbing and preloaded NOM interfered with MTBE adsorption. Preloaded NOM decreased the MTBE adsorption capacity to a greater extent than co-adsorbing NOM, which suggests that (1) preloaded NOM molecules occupied adsorption sites that were accessible to MTBE in the simultaneous loading experiment because the intraparticle diffusive flux of MTBE exceeded that of competing NOM molecules and/or (2) preloaded NOM molecules blocked access to pores in which MTBE adsorption sites are located. This result differs from that obtained by Hand et al. (1994), who did not observe any decrease in TCE adsorption capacity of the carbonaceous resin Ambersorb 563 after ten weeks of NOM exposure. This difference may be a result of differences in NOM characteristics. Hand et al. (1994) evaluated the preloading effect for a Wisconsin groundwater whereas the current study employed a North Carolina surface water. Furthermore, MTBE, which approximates a tetrahedron, is a bulkier molecule than the flat TCE molecule. Therefore, pore blockage effects may be more pronounced for MTBE than for TCE as previously shown by Quinlivan (2001).

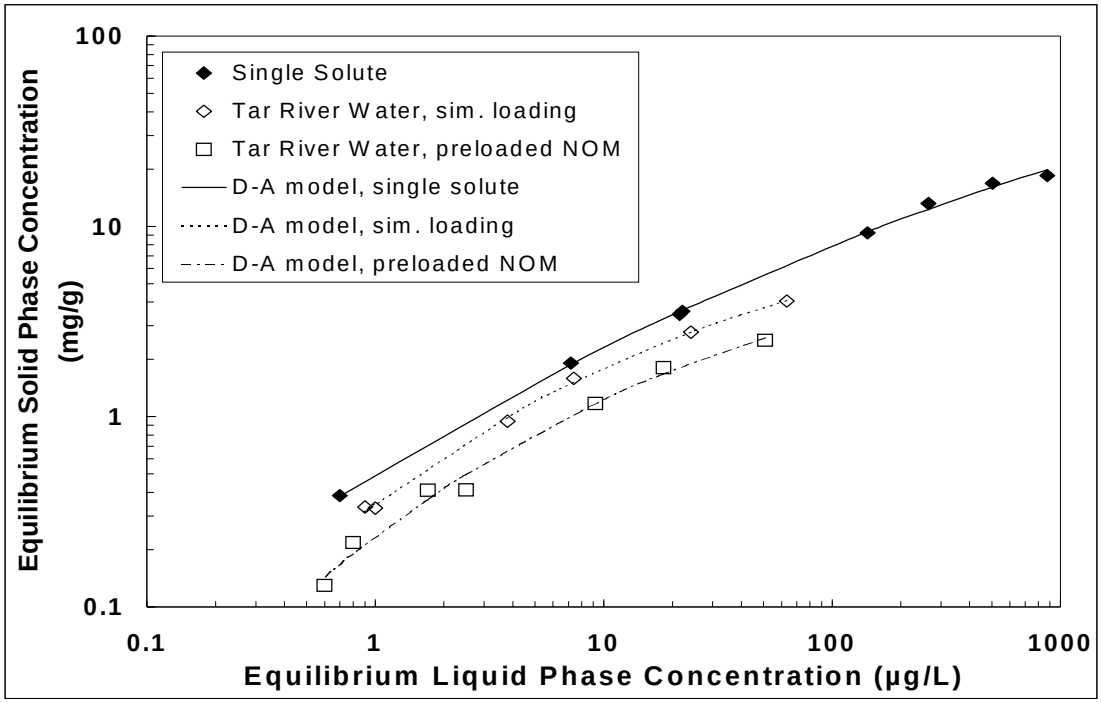


**Figure 16. Comparison of MTBE adsorption isotherms in ultrapure and Tar River water on carbonaceous resin Ambersorb 563. Lines represent Dubinin-Astakhov isotherm model fits.**

Figures 17 to 19 compare MTBE adsorption isotherms in ultrapure water and in the presence of co-adsorbing and preloaded NOM for three different activated carbons [CC-602, coconut shell-based carbon (Figure 17), UC-830, coal-based carbon (Figure 18), and F600, coal-based carbon (Figure 19)]. Figure 17 shows that NOM had little effect on the MTBE adsorption capacity of CC-602 at low liquid-phase concentrations; however, deviations between single-solute adsorption capacities and adsorption capacities in the presence of co-adsorbing and preloaded NOM were apparent at higher liquid phase concentrations (i.e., the data corresponding to the lower adsorbent doses). These results suggest that some pore blockage may have occurred in the presence of NOM at high NOM/adsorbent dose ratios.

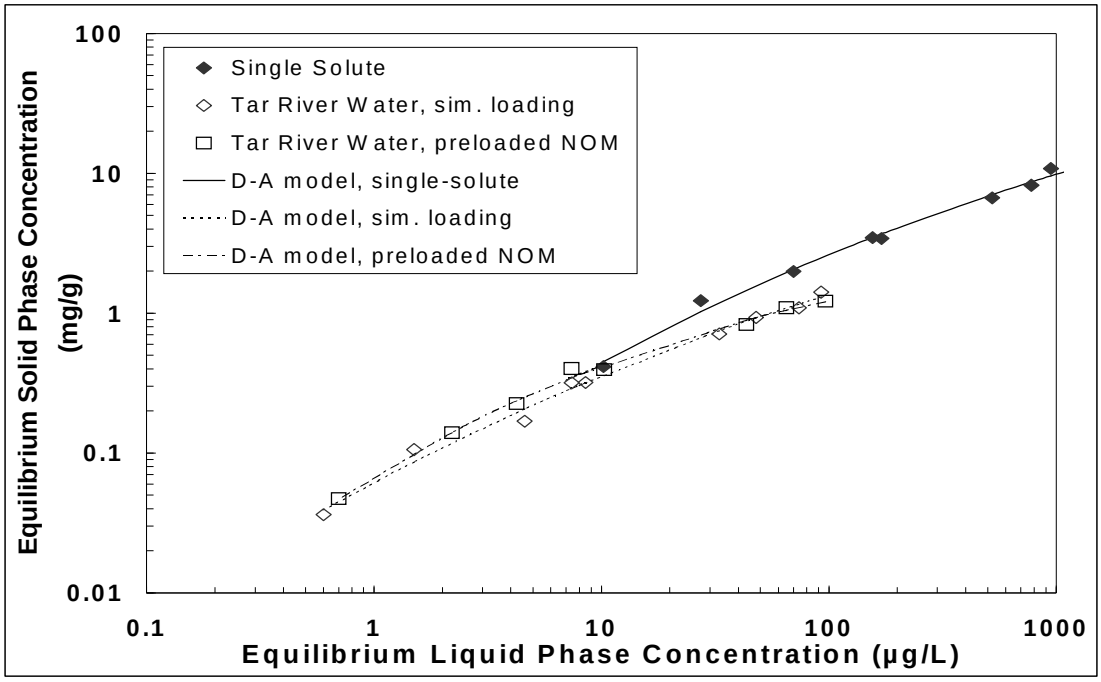


**Figure 17. Comparison of MTBE adsorption isotherms in ultrapure and Tar River water on activated carbon CC-602. Lines represent Dubinin-Astakhov isotherm model fits.**

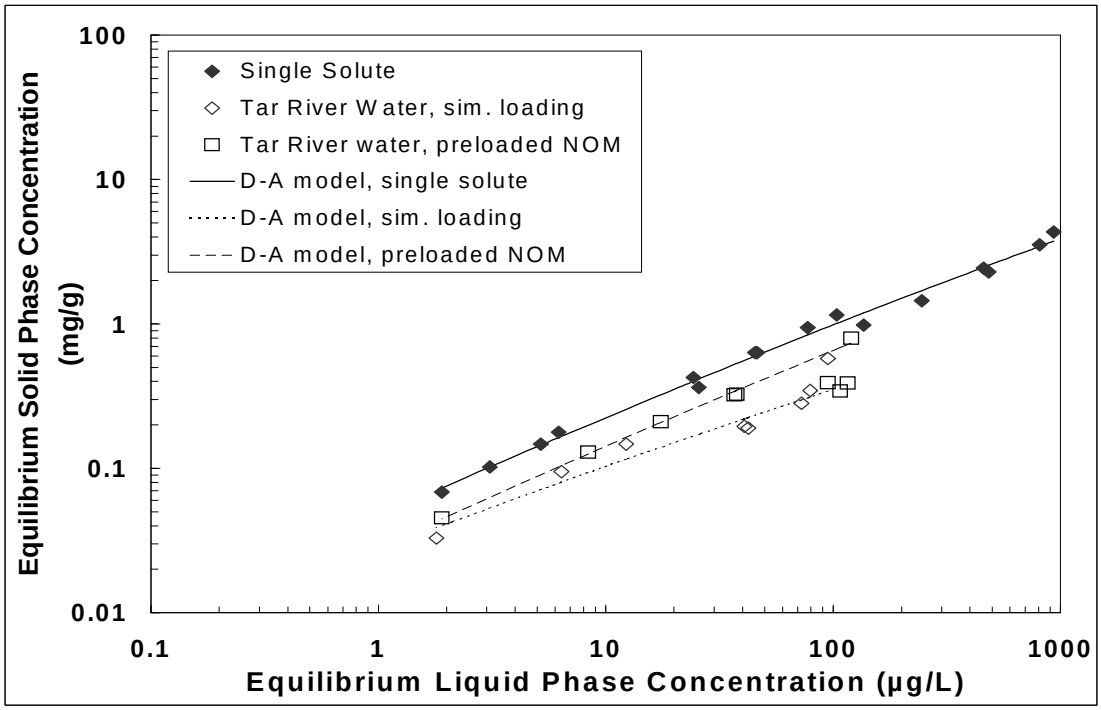


**Figure 18. Comparison of MTBE adsorption isotherms in ultrapure and Tar River water on activated carbon UC-830. Lines represent Dubinin-Astakhov isotherm model fits.**

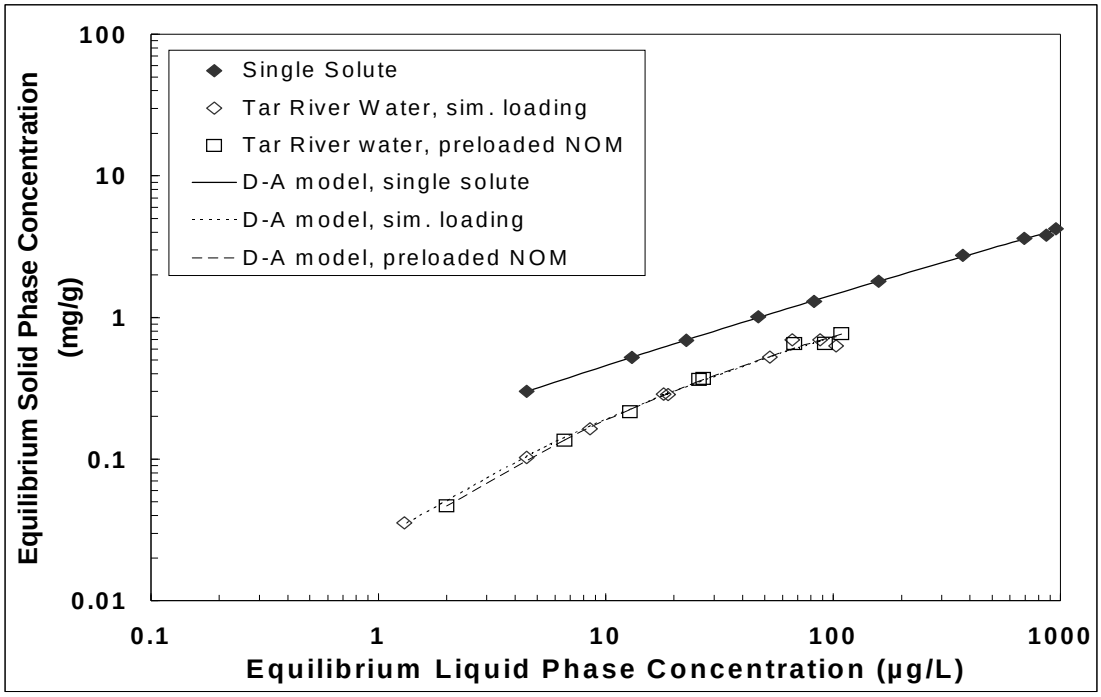


**Figure 19. Comparison of MTBE adsorption isotherms in ultrapure and Tar River water on activated carbon F600. Lines represent Dubinin-Astakhov isotherm model fits.**

Figures 18 and 19 compare MTBE adsorption isotherms in ultrapure water and TRW for the coal-based GACs UC-830 and F600, respectively. The data suggest that NOM lowered the MTBE adsorption capacity of these GACs more severely than those of the high-silica zeolites and the coconut shell-based activated carbon CC-602. Furthermore, the decrease in MTBE adsorption capacity over the entire range of liquid-phase MTBE concentrations suggests that NOM had access to the internal GAC pore structure, where it competed with MTBE for adsorption sites and/or blocked MTBE access to micropores.

### 4.4. Isotherm modeling

The DA isotherm model was used to describe experimental adsorption isotherm data and to compare MTBE adsorption capacities of the different adsorbents in organic-free water and Tar River water. The DA isotherm parameters and coefficients of determination ($R^2$) for the adsorbents discussed in section 4.3 are summarized in Table 4.

**Table 4. Dubinin-Astakhov isotherm parameters for selected adsorbents**

| Adsorbent | Condition | Dubinin-Astakhov isotherm parameters and coefficients of determination | | | |
|---|---|---|---|---|---|
| | | $q_m$ (mg/g) | E (kJ/mol) | n | $R^2$ |
| CBV-28014 ($NH_4^+$-ZSM-5) | Single-Solute | 244 | 21.6 | 2.79 | 0.9988 |
| | Sim. loading | 260 | 20.0 | 2.54 | 0.9989 |
| | Preloaded NOM | 243[(a)] | 21.1 | 2.70 | 0.9932 |
| SN-300 ($Na^+$-ZSM-5) | Single-Solute | 239 | 21.3 | 2.78 | 0.9998 |
| | Sim. loading | 240[(a)] | 20.8 | 2.65 | 0.9972 |
| | Preloaded NOM | 64 | 27.3 | 3.88 | 0.9982 |
| H-MFI-240 ($H^+$-ZSM-5) | Single-Solute | 123 | 23.3 | 3.10 | 0.9994 |
| | Sim. loading | 122[(a)] | 21.6 | 2.75 | 0.9970 |
| | Preloaded NOM | 122[(a)] | 22.1 | 2.81 | 0.9956 |
| HiSiv 3000 (Silicalite/ZSM-5) | Single-Solute | 342 | 18.9 | 2.37 | 0.9924 |
| | Sim. loading | 67 | 23.6 | 2.84 | 0.9965 |
| | Preloaded NOM | 341[(a)] | 17.1 | 2.12 | 0.9955 |
| HSZ-690HOA (Mordenite) | Single-Solute | 159 | 20.6 | 2.56 | 0.9884 |
| | Sim. loading | 2.7 | 38.1 | 6.19 | 0.9997 |
| | Preloaded NOM | 2.6 | 38.3 | 6.37 | 0.9993 |
| Ambersorb 563 (carb. resin) | Single-Solute | 107 | 21.9 | 2.41 | 0.9989 |
| | Sim. loading | 11.8 | 33.2 | 4.50 | 0.9981 |
| | Preloaded NOM | 8.3 | 33.1 | 4.48 | 0.9886 |
| CC-602 (Pulv. GAC) | Single-Solute | 69.5 | 20.9 | 2.68 | 0.9917 |
| | Sim. loading | 14.2 | 24.0 | 2.80 | 0.9908 |
| | Preloaded NOM | 3.3 | 32.7 | 4.57 | 0.9957 |
| UC-830 (Pulv. GAC) | Single-Solute | 317 | 9.4 | 1.41 | 0.9930 |
| | Sim. loading | 30[(a)] | 12.1 | 1.51 | 0.9546 |
| | Preloaded NOM | 326[(a)] | 8.5 | 1.36 | 0.9970 |
| F600 (Pulv. GAC) | Single-Solute | 130 | 11.2 | 1.41 | 0.9997 |
| | Sim. loading | 3.8 | 28.3 | 3.64 | 0.9937 |
| | Preloaded NOM | 3.3 | 29.4 | 3.99 | 0.9979 |

[(a)]: $q_m$ was fixed due to a poor convergence.

Single-solute n-values obtained for the zeolites, carbonaceous resin, and coconut-shell-based activated carbon ranged from about 2.4 to 3.1. This result is indicative of relatively homogeneous adsorbents with a narrow site energy distribution [Davis and Powers 2000]. In contrast, single-solute n-values for the coal-based activated carbons were approximately 1.4, a typical result that is indicative of more heterogeneous adsorbents with broader site energy distributions [Davis and Powers 2000].

A comparison of DA isotherm parameters obtained from MTBE isotherm data in ultrapure water and TRW shows that parameter estimates were similar in two cases (CBV-28014 and H-MFI-240) but quite different for the remaining adsorbents (Table 4). To better understand how changes in DA isotherm parameters affect isotherm position and shape, a sensitivity analysis was performed, in which each DA parameter was separately increased or decreased by 20% from the baseline values shown in Table 4. Figure 20 summarizes the results obtained for the ZSM-5 zeolite CBV-28014.

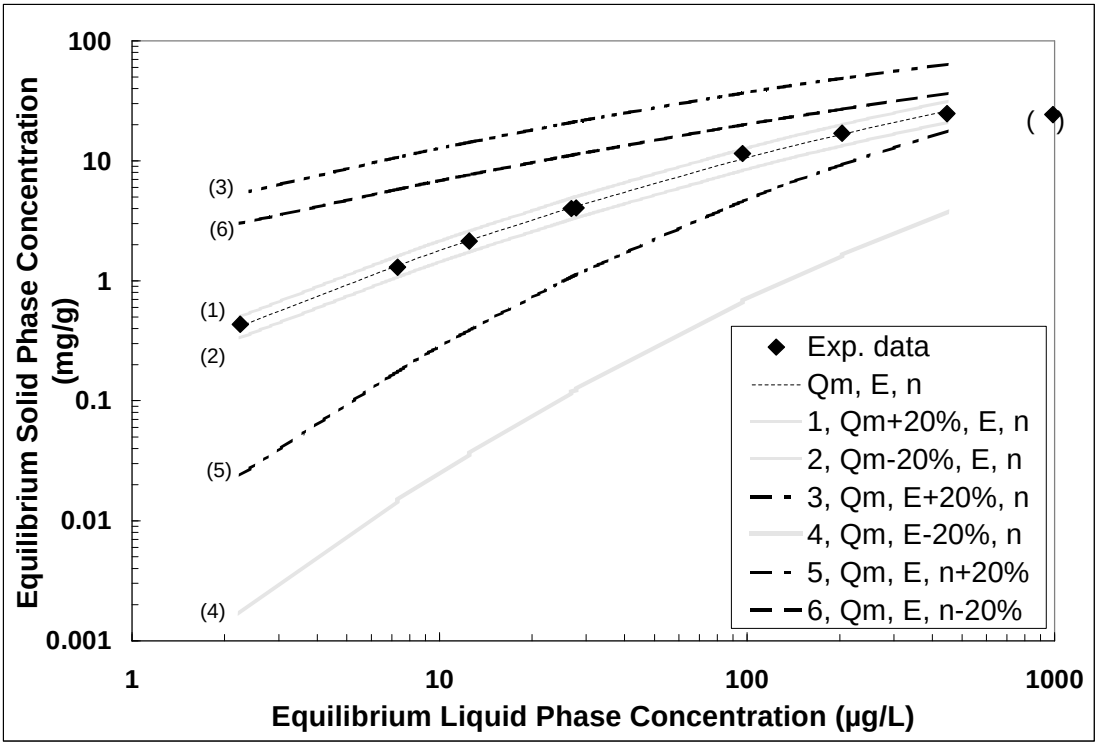


**Figure 20. Sensitivity analysis for DA isotherm parameters for the single-solute MTBE adsorption isotherm data collected with the ammonium-form ZSM-5 zeolite (CBV-28014). Data point in parenthesis was not included in analysis.**

Figure 20 shows that a 20% change in $q_m$ had a relatively small effect and resulted in a parallel translation of the entire isotherm in the q-direction, as expected. In contrast, 20% changes in E and n had a more dramatic effect on both isotherm shape and position. Given that in some instances all three DA parameters changed fairly dramatically when comparing the single-solute condition with the condition that incorporated NOM (see DA parameters for Mordenite, Ambersorb 563, F600 in Table 4), it is difficult to interpret these changes in a mechanistic manner. Additional analyses (e.g. $N_2$ adsorption isotherms on virgin and preloaded adsorbents to fix $q_m$, see e.g. Parker 1995) are required to evaluate whether any mechanistic information relative to NOM effects on MTBE adsorption is embedded in the DA isotherm parameters.

## 4.5. Practical implications

To evaluate the overall effectiveness of the tested adsorbents, the following analyses were made:

- MTBE adsorption capacities at an equilibrium liquid phase MTBE concentration of 10 µg/L ($q_{10}$) were compared for selected adsorbents using both the simultaneous MTBE/NOM loading and NOM preloading scenarios,
- The percent decrease in $q_{10}$ relative to the single-solute value was compared for the same adsorbents to assess the effect of NOM on MTBE adsorption capacity – this result may also affect the ease with which an adsorbent can be regenerated,
- Using the silicalite zeolite, the carbonaceous resin, and the three activated carbons, adsorbent usage rates (AURs) and costs associated with adsorbent usage were calculated and compared using a powdered adsorbent scenario and a granular adsorbent (packed bed) scenario, and
- Packed bed life was estimated and compared for the silicalite zeolite, the carbonaceous resin, and the three activated carbons.

### *4.5.1. Comparison of $q_{10}$ values*

MTBE adsorption capacities at an equilibrium liquid phase concentration of 10 µg/L ($q_{10}$) are compared in Table 5 for the simultaneous MTBE/NOM adsorption and the NOM preloading scenarios. The simultaneous MTBE/NOM loading scenario was chosen to represent a treatment condition, in which a powdered adsorbent is added to water while the NOM

preloading scenario was selected to simulate a condition that can be expected in the lower reaches of a packed-bed configuration. The latter scenario is obtained if the mass transfer zone for MTBE is shorter than that for NOM, in which case NOM adsorbs in the lower reaches of a packed bed adsorber prior to the arrival of the MTBE mass transfer zone. All $q_{10}$ values were calculated using the DA isotherm parameters shown in Table 4.

**Table 5. MTBE adsorption capacities at an equilibrium liquid phase concentration of 10 µg/L ($q_{10}$) in the presence of co-adsorbing or preloaded NOM and percent reductions in $q_{10}$ relative to single-solute values.**

| Adsorbent | $q_{10}$ AND % reduction of $q_{10}$ from single-solute value | | | |
|---|---|---|---|---|
| | Co-adsorbing NOM | | Preloaded NOM | |
| | $q_{10}$ (mg/g) | % reduction | $q_{10}$ (mg/g) | % reduction |
| CBV-28014 | 1.453 | 18.3[(a)] | 1.612 | 9.4[(b)] |
| SN-300 | 1.545 | 0.0[(b)] | 1.568 | 0.0[(b)] |
| H-MFI-240 | 0.962 | 17.4[(a)] | 1.136 | 2.5[(b)] |
| HiSiv 3000 | 1.295 | 22.8[(a)] | 1.317 | 21.4[(a)] |
| HSZ-690HOA | 0.965 | 22.7[(a)] | 0.958 | 23.2[(a)] |
| Ambersorb 563 | 1.792 | 22.0[(a)] | 1.223 | 46.7[(a)] |
| CC-602 | 0.355 | 20.1[(b)] | 0.419 | 5.7[(b)] |
| UC-830 | 0.103 | 54.0[(a)] | 0.142 | 36.7[(a)] |
| F600 | 0.191 | 58.2[(a)] | 0.188 | 58.8[(a)] |

[(a)]: significant difference ($p<0.05$)
[(b)]: no significant difference

In the case of co-adsorbing NOM, the carbonaceous resin exhibited the largest MTBE adsorption capacity ($q_{10}$) followed by the ZSM-5 zeolites SN-300 and CBV-28014 (Table 5). In the case of preloaded NOM, the ZSM-5 zeolites CBV-28014 and SN-300 exhibited the largest MTBE adsorption capacities. Among the activated carbons, the coconut-shell-based

CC-602 exhibited the highest MTBE adsorption capacity, but its $q_{10}$ value was only about 25% of that obtained for the ZSM-5 zeolites SN-300 and CBV-28014. The coal-based activated carbons exhibited the smallest MTBE adsorption capacities, and their $q_{10}$ values were approximately one order of magnitude smaller than those obtained for the ZSM-5 zeolites SN-300 and CBV-28014.

### *4.5.2. Effect of NOM on $q_{10}$*

The decrease in MTBE adsorption capacity ($q_{10}$) that resulted from co-adsorbed and preloaded NOM relative to the single-solute value ranged from about 0-23 % for the high-silica zeolites (Table 5). In several instances, the decrease in $q_{10}$ relative to the single-solute value was not statistically significant ($p < 0.05$) as shown in Table 5. These results suggest that NOM had either no or a small effect on MTBE adsorption for the high-silica zeolites presented in Table 5. Consequently, the SN-300 zeolite (and perhaps other silicalite/ZSM-5 zeolites) may perform well in packed bed adsorption systems because NOM preloading (fouling) effects are avoided or minimized. An absence of NOM fouling effects would further suggest that it is possible to regenerate high-silica zeolites with steam or microwave methods rather than with more energy-intensive thermal methods. Thermal regeneration is traditionally required for the regeneration of activated carbons that tend to adsorb large amounts of NOM in addition to the targeted trace organic contaminants.

The presence of NOM decreased the MTBE adsorption capacity of the coconut-shell-based activated carbon by percentages that were comparable to those obtained for the high-silica

zeolites (Table 5). However, as mentioned above, the MTBE adsorption capacity ($q_{10}$) of the coconut-shell-based activated carbon was 25% of that obtained for the high-silica zeolites SN-300 and CBV-28014. Also, as discussed in section 4.3, the MTBE isotherms collected with the coconut-shell-based activated carbon suggest that it may be more prone to experience pore blockage effects in the presence of NOM than the high silica zeolites (see Figure 17).

The MTBE adsorption capacities of the coal-based activated carbons UC-830 and F600 were severely affected by NOM presence, showing reductions in MTBE adsorption capacities of about 37-59% (Table 5). It should be noted that the MTBE adsorption capacity of the carbonaceous resin also decreased considerably (~47%) when NOM was preloaded. These results have important implications on resin and coal-based activated carbon performance in packed bed adsorbers because the results suggest that adsorbent fouling by preloaded NOM can be expected in the bottom reaches of the adsorber. Furthermore, NOM fouling of the coal-based activated carbons and the carbonaceous resin would affect regeneration options, which may be limited to thermal regeneration.

### *4.5.3. Adsorbent usage rates and associated costs*

To further evaluate the feasibility of employing high-silica zeolites for MTBE removal, a simple cost analysis based on adsorbent usage rates was performed. An important cost in the operation of adsorption systems is the cost of the adsorbent itself. Apart from affecting cost, high adsorbent usage rates may also pose other practical problems such as (i) a treatment

plant's inability to feed a powdered adsorbent at the required rate or (ii) an excessively high replacement frequency of granular adsorbents in packed bed adsorbers. The adsorbent usage rate and cost analysis was performed for one readily available, relatively economical zeolite (HiSiv3000, cost ~$7/lb, Price and Schmidt 1998, Hajdu 2000), the carbonaceous resin (Ambersorb 563, cost ~$35/lb, Melin 1999), and three activated carbons (CC-602, UC-830, F-600, cost ~$1.50/lb, Melin 1999).

Two scenarios were considered: (1) use of powdered adsorbent to treat water with an initial MTBE concentration of 50 µg/L and a treatment goal of 5 µg/L (the California standard), and (2) use of granular adsorbent in a packed bed system to treat water with the same initial MTBE concentration. For both scenarios, it was assumed that equilibrium is obtained. Furthermore, for the packed bed configuration, it was assumed that the effluent MTBE concentration is zero. The equations used to calculate the adsorbent usage rate (AUR) are:

$$For\ scenario\ 1: AUR = \frac{C_0 - C_{eff}}{q_{@\,C_{eff}}} \qquad \text{(eq. 5)}$$

$$For\ scenario\ 2: AUR = \frac{C_0}{q_{@\,C_{inf}}} \qquad \text{(eq. 6)}$$

where $C_0$ is the influent MTBE concentration (50 µg/L), $C_{eff}$ is the effluent MTBE concentration (5 µg/L for scenario 1), and $q_{@Ceff}$ and $q_{@Cinf}$ are the MTBE adsorption capacities at the effluent and influent liquid phase concentrations, respectively. MTBE adsorption capacities were calculated using the simultaneous loading condition DA parameters for the powdered adsorbent scenario and the preloaded NOM condition DA parameters for the packed bed scenario (Table 4).

Costs associated with adsorbent usage were based on the treatment of 1000 gal of water. Table 6 summarizes AURs and associated costs for the five adsorbents. For scenario 1, the coconut-shell-based activated carbon (CC-602) was the most economical option followed by the silicalite zeolite (HiSiv 3000), which was approximately 30% more expensive. The most costly option was the carbonaceous resin (Ambersorb 563) despite the fact that it had the lowest AUR. For scenario 2, the most economical options were the silicalite zeolite (HiSiv 3000) and the coconut-shell-based activated carbon (CC-602) with the same cost of $0.7/1000 gallons treated. Although the cost for these two adsorbents was similar, the zeolite may be a more reasonable option because its AUR is only 23% of that associated with CC-602. As a result, adsorbent replacement would have to occur on a less frequent basis in the zeolite-based adsorber (see also section 4.5.4). Again, the carbonaceous resin was the most costly option with a cost $5.7 per 1000 gallons treated.

**Table 6. Adsorbent usage rates and associated costs.**

| Adsorbent | Scenario 1: Powdered Adsorbent | | Scenario 2: Packed Bed Adsorber | |
|---|---|---|---|---|
| | AUR (mg/L) | Cost ($/1000 gal) | AUR (mg/L) | Cost ($/1000 gal) |
| **HiSiv 3000** | 59 | 3.4 | 12 | 0.7 |
| **Ambersorb 563** | 38 | 11.1 | 19 | 5.7 |
| **CC-602** | 205 | 2.6 | 53 | 0.7 |
| **UC-830** | 643 | 8.0 | 120 | 1.5 |
| **F600** | 395 | 5.0 | 96 | 1.2 |

### *4.5.4. Packed bed life*

One important aspect in the operation of packed bed adsorbers is the frequency with which adsorbent needs to be replaced or regenerated. Using the AURs shown in Table 6 and the bed

density ($\rho_{bed}$) for the different adsorbents, estimates of packed bed life were calculated for an adsorber with an assumed empty bed contact time (EBCT) of 15 minutes with the following equations:

$$BV = \frac{r_{bed}\left(g/cm^3\right)}{AUR\left(mg/L\right)} * \frac{1000\ mg}{g} * \frac{1000\ cm^3}{L} \qquad \text{(eq. 7)}$$

$$Adsorber\ Life\left(d\right) = EBCT\ \left(\min\right) * BV * \frac{1\ d}{1440\ min} \qquad \text{(eq. 8)}$$

where BV is the number of bed volumes that can be treated to fully utilize the adsorbent's MTBE adsorption capacity. Table 7 summarizes the bed densities, BV values, and adsorber life estimates for the selected adsorbents.

**Table 7. Estimated adsorber life for selected adsorbents**

| Adsorbent | $\rho_{bed}$ ($g/cm^3$) | BV | Adsorber life (d) for EBCT=15 min |
|---|---|---|---|
| HiSiv 3000 | 0.7 | 58,700 | 612 |
| Ambersorb 563 | 0.53 | 27,300 | 285 |
| CC-602 | 0.5 | 9430 | 98 |
| UC-830 | 0.5 | 4180 | 43 |
| F600 | 0.6 | 6240 | 65 |

As shown in Table 7, adsorber life estimates ranged from about 1.5-3 months for the GACs to about 20 months for the HiSiv3000 zeolite. For the carbonaceous resin, the adsorber life was estimated to be about 9 months. Based on the cost analysis presented in Table 6, both the CC-602 GAC and the HiSiv 3000 zeolite options resulted in similar costs related to adsorbent usage. However, the results in Table 7 suggest that adsorbent replacement/regeneration of the CC-602 GAC would have to take place approximately every 3 months while adsorbent

replacement/regeneration of the HiSiv3000 zeolite would have to take place approximately every 20 months. It should be noted here that in addition to a higher MTBE adsorption capacity on a unit mass basis, the high-silica zeolite offers the advantage of a higher bed density ($\rho_{bed}$ = 0.7 g/cm$^3$) than most GACs ($\rho_{bed}$ = 0.5 g/cm$^3$). As a result, a greater adsorbent mass can be placed in an adsorber of a given volume, which extends packed bed life further than what would be predicted from a comparison of AURs. Thus, adsorbent replacement/regeneration has to occur on a much less frequent basis with the HiSiv3000 zeolite compared with the CC-602 GAC. As mentioned previously, it may be possible to regenerate spent high-silica zeolite with steam or microwave methods rather than with more energy-intensive thermal methods. This opportunity may further lower the costs of a zeolite-based adsorption system for MTBE removal from water.

## 5. CONCLUSIONS

MTBE adsorption isotherm data were collected for a matrix of high-silica zeolites with different pore sizes (ZSM-5/silicalite, Mordenite, Beta, Y), exchangeable cations ($H^+$, $Na^+$, $NH_4^+$), and hydrophobicities ($SiO_2/Al_2O_3$ ratios). MTBE adsorption capacities of high-silica zeolites were compared to those of three GACs (one coconut-shell-based, two coal-based) and a carbonaceous resin (Ambersorb 563). Single-solute isotherm tests were conducted in ultrapure water buffered at pH 7.2. Additional isotherm studies were conducted to determine the effects of co-adsorbing and preloaded NOM on MTBE adsorption from Tar River water (Greenville, NC). Based on the experimental data, the following conclusions were drawn:

- Single-solute MTBE adsorption isotherm data showed that high-silica zeolites with smaller pores (ZSM-5/silicalite, Mordenite) were more effective adsorbents for MTBE than zeolites with somewhat larger pores (Beta, Y).

- No clear dependence of MTBE adsorption capacity on zeolite $SiO_2/Al_2O_3$ ratio was obtained for ZSM-5/silicalite zeolites with $SiO_2/Al_2O_3$ ratios in the range of 90 to 700. This result suggests that water cluster formation is difficult inside the ZSM-5/silicalite pores over the tested $SiO_2/Al_2O_3$ range. Small, hydrophobic pores can disrupt hydrogen bonds of water to the extent that a continuous liquid water phase likely was not present inside of the zeolites pores.

- The exchangeable cation ($H^+$, $Na^+$, $NH_4^+$) of high-silica ZSM-5 zeolites had little effect on MTBE adsorption at the tested conditions, and no zeolite-catalyzed MTBE hydrolysis was apparent for ZSM-5 zeolites in the $H^+$ form.

- For high-silica zeolites, co-adsorbing and preloaded NOM lowered the single-solute MTBE adsorption capacity at a liquid-phase MTBE concentration of 10 µg/L ($q_{10}$) by 0-23%. Similar decreases in MTBE adsorption capacity as a result of NOM adsorption were measured for the coconut-shell-based activated carbon CC-602; however, its MTBE adsorption capacity ($q_{10}$) was only about 25% of that obtained for ZSM-5 zeolites. In the presence of preloaded NOM, the MTBE adsorption capacity of the carbonaceous resin ($q_{10}$) decreased by about 47% relative to the single-solute value while that of one coal-based activated carbon decreased by almost 60%. Overall, the coal-based activated carbons exhibited the smallest MTBE adsorption capacities ($q_{10}$), which were approximately one order of magnitude lower than those of the ZSM-5 zeolites.

- Based on equilibrium model calculations, the lowest treatment cost for a packed bed adsorption system ($0.7/1000 gal) was associated with the usage of HiSiv3000 zeolite (cost: ~$7/lb) and CC-602 GAC (cost: ~1.50/lb). Although the cost for these two adsorbents was similar, the zeolite-based adsorption system may be more advantageous because (1) the adsorbent usage rate calculated for the HiSiv3000 zeolite was less than 25% of that calculated for the CC-602 GAC and (2) the calculated bed life for a packed bed adsorber containing HiSiv3000 zeolite was more than 6 times longer than that for an equally sized packed bed adsorber containing CC-602 GAC, a result that was affected by

the lower packed bed density of the latter adsorbent. Thus, adsorbent replacement/ regeneration would have to occur on a less frequent basis when zeolites are used.

- Future work is required to measure MTBE adsorption kinetics on high-silica zeolites and to evaluate the potential of regenerating high-silica zeolites using steam.

## 6. REFERENCES


Acero, J.L., S.B. Haderlein, T.C. Schmidt, M.J.F. Suter, and U. von Gunten. 2001. "MTBE Oxidation by Conventional Ozonation and the Combination Ozone/Hydrogen Peroxide: Efficiency of the Processes and Bromate Formation". *Environmental Science and Technology.* **35**(21): 4252-4259.

Anderson, M.A. 2000. "Removal of MTBE and Other Organic Contaminants from Water by Sorption to High Silica Zeolites." *Environmental Science and Technology* **34**(4): 725-727.

AWWA E-MainStream (2004). "MTBE at a Glance". http://www.awwa.org/communications/mainstream/2004/Mar16/sidebars/MTBEfacts.cfm. Accessed June 4, 2004.

California EPA (1999). "Public Health Goal for Methyl Tertiary Butyl Ether (MTBE) in Drinking Water". Office of Environmental Health Hazard Assessment, Sacramento, CA. Available at: http://www.oehha.ca.gov/water/phg/allphgs.html. Accessed June 4, 2004.

Carrott, P.J.M.; Kenny, M.B.; Roberts, R.A.; Sing, K.S.W.; and Theocharis C.R. 1991. "The adsorption of water vapour by microporous solids. In *Characterization of Porous Solids II. Studies in Surface Science and Catalysis*, vol. **62**, F. Rodriguez-Reinoso et al., eds. Elsevier Sicence Publishers, Amsterdam, pp. 685-692.

Centi, G. and S. Perathoner. 2003. "Remediation of water contamination using catalytic technologies". *Applied Catalysis B-Environmental*. **41**(1-2): 15-29.

Centi, G.; Grande, A.; and S. Perathoner. 2002. "Catalytic conversion of MTBE to biodegradable chemicals in contaminated water." *Catalysis Today*. **75**: 69-76.

Davis, S.W. and S.E. Powers. 2000. "Alternative Sorbents for Removing MTBE from Gasoline-Contaminated Ground Water". *Journal of Environmental Engineering*. **126** (4): 354-360.

Deeb, R.A., Chu, K., Shih, T., Linder, S., Suffet, I., Kavanaugh, M.C., and L. Alvarez-Cohen. 2003. "MTBE and Other Oxygenates: Environmental Sources, Analysis, Occurrence, and Treatment". *Environmental Engineering Science.* **20**(5): 433-447.

Draper, N.R. and H. Smith. 1981. *Applied Regression Analysis.* John Wiley & Sons, Inc. USA.

Giaya, A. and R.W. Thompson. 2002. "Water confined in cylindrical micropores." *Journal of Chemical Physics.* **117**(7): 3464-3475.

Giaya, A.; Thompson, R.W.; and R. Denkewicz, Jr. 2000. "Liquid and vapor phase adsorption of chlorinated volatile organic compounds on hydrophobic molecular sieves." *Microporous and Mesoporous Materials.* **40**: 205-218.

Hajdu, D. 2000. Personal Communication, UOP Molecular Sieves, Mt. Laurel, NJ.

Hand, D.W., Herlevich Jr., J.A., Perram, D.L., and J.C. Crittenden. 1994. "Synthetic adsorbent versus GAC for TCE removal". *Journal of the American Water Works Association.* **86**(8): 64-72.

Interagency Oxygenated Fuels Assessment Steering Committee (1997). Interagency assessment of oxygenated fuels. National Science and Technology Council, Committee on Environment and Natural Resources and Office of Science and Technology Policy. Washington, DC. Available at: http://www.epa.gov/otaq/fuels.htm#oxy. Accessed June 4, 2004.

Johnson, R., J. Pankow, D. Bender, C. Price, and J. Zogorski. 2000. "MTBE – To What Extent Will Past Releases Contaminate Community Water Supply Wells?" *Environmental Science and Technology*, May 1, 2A-9A.

Kawai, T., Yanagihara, T., and K. Tsutsumi. 1994. "Adsorption characteristics of chloroform on modified zeolites from gaseous phase as well as its aqueous solution". *Colloid & Polymer Science.* **272**: 1620-1626.

Kenny, M.B. and K.S.W. Sing. 1990. "The hydrophobicity of Silicalite and ZSM-5". *Chemistry & Industry*. Pp. 39-40.

Kilduff, J.E and T. Karanfil. 2002. “Trichloroethylene adsorption by activated carbon preloaded with humic substances: effects of solution chemistry.” *Water Research.* **36**: 1685-1698.

Kilduff, J.E., Karanfil, T., and W.J. Weber Jr. 1998. “Competitive Effects of Nondisplaceable Organic Compounds on Trichloroethylene Uptake by Activated Carbon. I. Thermodynamic Predictions and Model Sensitivity Analyses”. *Journal of Colloid and Interface Science.* **205**: 271-279.

Lamberth, R. 2004. “2003 was a year of transition for the MTBE, fuels industry”. *Oil & Gas Journal.* **102**(2): 52-58.

Leitner, N.K.V., A.L. Papailhou, J.P. Croue, J. Peyrot, and M. Dore. 1994. “Oxidation of Methyl Tert-Butyl Ether by Ozone and Combined Ozone Hydrogen-Peroxide.” *Ozone Science and Engineering* **16**(1): 41-54.

Li, L.; Quinlivan, P.A.; and Knappe, D.R.U. 2002. “Effects of Activated Carbon Surface Chemistry and Pore Structure on the Adsorption of Organic Contaminants from Aqueous Solution.” *Carbon*, **40** (12): 2085-2100

Li, S.; Tuan, V.A.; Noble, R.D.; and Falconer, J.L. 2003a. “MTBE Adsorption on all-silica ß zeolite.” *Environmental Science and Technology* **37**(17): 4007-4010.

Li, Q., Snoeyink, V.L., Mariãas, B.J., and C. Campos. 2003b. “Elucidating competitive adsorption mechanisms of atrazine and NOM using model compounds”. *Water Research.* **37**: 773-784.

Liang, S., L.S. Palencia, R.S. Yates, M.K. Davis, J.M. Bruno, and R.L. Wolfe. 1999. “Oxidation of MTBE by Ozone and Peroxone Processes.” *Journal AWWA* **91**(6): 104-114.

Lichtblau, J., L. Goldstein, and R. Gold. 2004. “MTBE issues include Question of all Oxygenate Mandates”. *Oil & Gas Journal.* **102** (12): 18-26.

McCusker, L.B. and C Baerlocher. 2001. “Zeolite Structures”. In *Introduction to Zeolite Science and Practice, 2nd Completely Revised and Expanded Edition*, van Bekkum, H.,

E.M. Flanigen, P.A. Jacobs, and J.C. Jansen, eds. Elsevier Science, Amsterdam, pp. 37-67.

Meier, W.M. and C. Baerlocher. 1998. "Zeolite Type Frameworks: Connectivities, Configurations and Conformations". In *Molecular Sieves: Science and Technology*, vol. 2, Karge, H.G. and J. Weitkamp, eds. Springer-Verlag, Berlin, pp. 139-161.

Melin, G. 1999. *Evaluation of the Applicability of Synthetic Resin Sorbents for MTBE Removal from Water.* The California MTBE Research Partnership. National Water Research Institute, Fountain Valley, CA.

Mormile, M.R., S. Liu, and J.M. Suflita. 1994. "Anaerobic Biodegradation of Gasoline Oxygenates: Extrapolation of Information to Multiple Sites and Redox Conditions." *Environmental Science and Technology* **28**(9): 1727-1732.

Parker, G.R. 1995. "Optimum Isotherm Equation and Thermodynamic Interpretation for Aqueous 1,1,2-Trichloroethene Adsorption Isotherms on Three Adsorbents". *Adsorption* **1**: 113-132.

Pelekani, C. and V.L. Snoeyink. 1999. "Competitive Adsorption in Natural Water: Role of Activated Carbon Pore Size". *Water Research.* **33**(5): 1209-1219.

Pfenninger, A. 1998. "Manufacture and Use of Zeolites for Adsorption Processes". In *Molecular Sieves: Science and Technology*, vol. 2, Karge, H.G. and J. Weitkamp, eds. Springer-Verlag, Berlin, pp. 163-198.

Price, D.W. and P.S. Schmidt. 1998. "VOC Recovery through Microwave Regeneration of Adsorbents: Process Design Studies." *Journal of the Air and Waste Management Association* **48**(12): 1135-1145.

Quinlivan, 2001. "Effects of activated carbon surface chemistry and pore structure on the adsorption of methyl tertiary-butyl ether and trichloroethene from natural water". M.S. Thesis. North Carolina State University. http://www.lib.ncsu.edu/etd/public/etd-2751711610131911/etd.pdf

Ramakrishnan, B., Sorial, G.A., Speth, T.F., Clark, P., Zaffiro, A., Patterson, C., and D.W. Hand. 2004. "Remediation of MTBE from Drinking Water: Air Stripping Followed by

Off-Gas Adsorption". *Journal of the Air & Waste Management Association.* **54**: 529-539.

Rouquerol, F., J. Rouquerol, and K. Sing. 1999. *Adsorption by Powders and Porous Solids*. Academic Press, San Diego, CA.

Shih, T.C., Wangpaichitr, M., and M. Suffet. 2003. "Evaluation of granular activated carbon technology for the removal of methyl tertiary butyl ether (MTBE) from drinking water". *Water Research.* **37**: 375-385.

Squillace, P.J., J.F. Pankow, N.E. Korte, and J.S. Zogorski. 1997. "Review of the Environment Behavior and fate of Methyl tert-butyl Ether". *Environmental Toxicology and Chemistry.***16** (9): 1836-1844.

Stocking, A.J., Suffet, I.H., McGuire, M.J., and M.C. Kavanaugh. 2001. "Implications of an MTBE odor study for setting drinking water standards". *Journal of American Water Works Association.* **93**(3): 95-105.

Stumm, W. and Morgan, J.J. *Aquatic Chemistry*. 1996. John Wiley & Sons, Inc.: New York, NY. (see Figure 15.1)

Sutherland, J., Adams, C., and J. Kekobad. 2004. "Treatment of MTBE by air stripping, carbon adsorption, and advanced oxidation: technical and economic comparison for five groundwaters". *Water Research.* **38**: 193-205.

Szostak, R. 1992. "Handbook of Molecular Sieves". Van Nostrand Reinhold, New York. U.S.A.

Szostak, R. 1998. "Molecular Sieves". Internation Thomson Publishing, London, United Kingdom.

U.S. Department of Health and Human Services (2002). National Toxicology Program. "Tenth Report on Carcinogens". Public Health Service, Washington, DC. Available at: http://ehp.niehs.nih.gov/roc/toc10.html#toc. Accessed June 4, 2004.

U.S. EPA (1994a). "Health Risk Perspectives on Fuel Oxygenates". Report no. EPA/R-94/217. Office of Research and Development, Washington, DC. Available at: http://www.epa.gov/ncea/oxygenates/risk-oxy.htm. Accessed June 4, 2004.

U.S. EPA. (1994b). "Chemical Summary for Methyl-Tert-Butyl Ether". Report no. EPA-749-F-94-017a. Office of Pollution Prevention and Toxics, Washington, DC.

U.S. EPA (1997). "Drinking Water Advisory: Consumer Acceptability Advice and Health Effects Analysis on Methyl Tertiary-Butyl Ether (MTBE)". Report no. EPA-822-F-97-008. Office of Water, Washington, DC. Available at: http://www.epa.gov/ost/drinking/mtbe.html. Accessed June 4, 2004.

U.S. EPA (2003). "Methyl Tertiary Butyl Ether (MTBE)". http://www.epa.gov/mtbe/gas.htm. Accessed June 4, 2004.

USGS. 1996. *Occurrence of the Gasoline Additive MTBE in Shallow Ground Water in Urban and Agricultural Areas.* United States Geological Survey Fact Sheet 114.95.

Wilhelm, M.J., Adams, V.D., Curtis, J.G., and E.J. Middlebrooks. 2002. "Carbon Adsorption and Air-stripping Removal of MTBE from River Water". *Journal of Environmental Engineering.* **128**(9): 813-823.

World Health Organization (1998). "Methyl tertiary-butyl ether". *Environmental Health Criteria 206*. World Health Organization, Geneva, Switzerland.

Young, W.F., H. Horth, R. Crane, T. Ogden, and M. Arnott. 1996. "Taste and Odour Threshold Concentrations of Potential Potable Water Contaminants". *Water Research.***30** (2): 331-340.

# APPENDICES

## Appendix A. Raw data for single-solute MTBE isotherms

**Table A.1. Single-solute MTBE adsorption isotherm on ZSM-5 zeolite CBV-28014 ($NH_4^+$ form)**

**Adsorbent Type: Zeolite ZSM-5 (CBV 28014)**
**Solvent: buffered ultrapure water at pH 7.2**
**Micropollutant: MTBE**

| Solvent Volume (mL) | Weight of Zeolite (mg) | Zeolite Conc. (mg/L) | Initial MTBE Conc. (µg/L) | MTBE Conc. (µg/L) | Qe (mg/g) |
|---|---|---|---|---|---|
| 495 | 5.0 | 10.10 | 1232.6 | 987.1 | 24.31 |
| 495 | 15.7 | 31.72 | 1232.6 | 446.6 | 24.78 |
| 495 | 30.0 | 60.61 | 1232.6 | 203.7 | 16.98 |
| 252 | 24.9 | 98.81 | 1232.4 | 96.7 | 11.49 |
| 252 | 74.9 | 297.22 | 1232.4 | 27.8 | 4.05 |
| 252 | 75.9 | 301.19 | 1232.4 | 26.8 | 4.00 |
| 126.8 | 75.4 | 594.64 | 1286.7 | 12.5 | 2.14 |
| 126.8 | 124.9 | 985.02 | 1286.7 | 7.3 | 1.30 |
| 126.8 | 374.7 | 2955.05 | 1286.7 | 2.2 | 0.43 |

**Table A.2. Single-solute MTBE adsorption isotherm without buffer on ZSM-5 zeolite CBV-28014 ($NH_4^+$ form)**

**Adsorbent Type: Zeolite ZSM-5 (CBV 28014)**
**Solvent: ultrapure water without buffer**
**Micropollutant: MTBE**

| Solvent Volume (mL) | Weight of Zeolite (mg) | Zeolite Conc. (mg/L) | Initial MTBE Conc. (µg/L) | MTBE Conc. (µg/L) | Qe (mg/g) |
|---|---|---|---|---|---|
| 252 | 14.8 | 58.73 | 1117.1 | 182.40 | 15.91 |
| 252 | 26.1 | 103.57 | 1117.1 | 93.86 | 9.88 |
| 252 | 76.7 | 304.37 | 1117.1 | 27.19 | 3.58 |
| 252 | 76.2 | 302.38 | 1117.1 | 26.32 | 3.61 |
| 252 | 151.2 | 600.00 | 1117.1 | 12.28 | 1.84 |

**Table A.3. Single-solute MTBE adsorption isotherm on ZSM-5 zeolite SN-300 ($Na^+$ form)**

**Adsorbent Type: Zeolite ZSM-5 (SN-300)**
**Solvent: buffered ultrapure water at pH 7.2**
**Micropollutant: MTBE**

| Solvent Volume (mL) | Weight of Zeolite (mg) | Zeolite Conc. (mg/L) | Initial MTBE Conc. (µg/L) | MTBE Conc. (µg/L) | Qe (mg/g) |
|---|---|---|---|---|---|
| 495 | 5.4 | 10.91 | 1100.8 | 764.89 | 30.79 |
| 495 | 16.7 | 33.74 | 1100.8 | 377.30 | 21.44 |
| 495 | 29.8 | 60.20 | 1100.8 | 191.00 | 15.11 |
| 252 | 24.9 | 98.81 | 1116.3 | 113.00 | 10.15 |
| 252 | 74.2 | 294.44 | 1116.3 | 28.90 | 3.69 |
| 252 | 77.0 | 305.56 | 1116.3 | 27.10 | 3.56 |
| 126.8 | 76.5 | 603.31 | 1175.2 | 13.30 | 1.93 |
| 126.8 | 124.5 | 981.86 | 1175.2 | 7.80 | 1.19 |
| 126.8 | 377.8 | 2979.50 | 1175.2 | 2.50 | 0.39 |

**Table A.4. Single-solute MTBE adsorption isotherm without buffer on ZSM-5 zeolite SN-3000 ($Na^+$ form)**

**Adsorbent Type: Zeolite ZSM-5 (SN-300)**
**Solvent: ultrapure water without buffer**
**Micropollutant: MTBE**

| Solvent Volume (mL) | Weight of Zeolite (mg) | Zeolite Conc. (mg/L) | Initial MTBE Conc. (µg/L) | MTBE Conc. (µg/L) | Qe (mg/g) |
|---|---|---|---|---|---|
| 495 | 5.5 | 11.11 | 1054.3 | 701.31 | 31.77 |
| 495 | 15.7 | 31.72 | 1054.3 | 329.83 | 22.84 |
| 495 | 30.8 | 62.22 | 1054.3 | 150.88 | 14.52 |
| 252 | 25.4 | 100.79 | 1072.7 | 85.09 | 9.80 |
| 252 | 75.1 | 298.02 | 1072.7 | 23.68 | 3.52 |
| 252 | 76.1 | 301.98 | 1072.7 | 23.68 | 3.47 |
| 126.8 | 75.4 | 594.64 | 1112.0 | 12.10 | 1.85 |
| 126.8 | 126.8 | 1000.00 | 1112.0 | 6.80 | 1.11 |
| 126.8 | 375.2 | 2958.99 | 1112.0 | 2.20 | 0.38 |

**Table A.5. Single-solute MTBE adsorption isotherm on ZSM-5 zeolite H-MFI-240 ($H^+$ form)**

**Adsorbent Type: Zeolite ZSM-5 (H-MFI-240)**
**Solvent: buffered ultrapure water at pH 7.2**
**Micropollutant: MTBE**

| Solvent Volume (mL) | Weight of Zeolite (mg) | Zeolite Conc. (mg/L) | Initial MTBE Conc. (µg/L) | MTBE Conc. (µg/L) | Qe (mg/g) |
|---|---|---|---|---|---|
| 495 | 4.8 | 9.70 | 1175.4 | 936.0 | 24.68 |
| 495 | 14.7 | 29.70 | 1175.4 | 580.2 | 20.04 |
| 495 | 29.8 | 60.20 | 1175.4 | 283.3 | 14.82 |
| 252 | 25.0 | 99.21 | 1189.7 | 177.2 | 10.21 |
| 252 | 74.7 | 296.43 | 1189.7 | 42.5 | 3.87 |
| 252 | 76.0 | 301.59 | 1189.7 | 41.2 | 3.81 |
| 126.8 | 75.5 | 595.43 | 1264.7 | 18.4 | 2.09 |
| 126.8 | 125.6 | 990.54 | 1264.7 | 11.2 | 1.27 |
| 126.8 | 376.6 | 2970.03 | 1264.7 | 3.6 | 0.42 |

**Table A.6. Single-solute MTBE adsorption isotherm without buffer on ZSM-5 zeolite H-MFI-240 ($H^+$ form)**

**Adsorbent Type: Zeolite ZSM-5 (H-MFI-240)**
**Solvent: ultrapure water without buffer**
**Micropollutant: MTBE**

| Solvent Volume (mL) | Weight of Zeolite (mg) | Zeolite Conc. (mg/L) | Initial MTBE Conc. (µg/L) | MTBE Conc. (µg/L) | Qe (mg/g) |
|---|---|---|---|---|---|
| 252 | 15.7 | 62.30 | 1117.1 | 251.31 | 13.90 |
| 252 | 26.0 | 103.17 | 1117.1 | 131.58 | 9.55 |
| 252 | 76.3 | 302.78 | 1117.1 | 32.46 | 3.58 |
| 252 | 75.0 | 297.62 | 1117.1 | 32.46 | 3.64 |
| 252 | 150.8 | 598.41 | 1117.1 | 14.04 | 1.84 |

**Table A.7. Single-solute MTBE adsorption isotherm on silicalite zeolite HiSiv 3000**

**Adsorbent Type: Zeolite ZSM-5/silicalite (HiSiv 3000)**
**Solvent: buffered ultrapure water at pH 7.2**
**Micropollutant: MTBE**

| Solvent Volume (mL) | Weight of Zeolite (mg) | Zeolite Conc. (mg/L) | Initial MTBE Conc. (µg/L) | MTBE Conc. (µg/L) | Qe (mg/g) |
|---|---|---|---|---|---|
| 495 | 4.8 | 9.70 | 1181.7 | 917.90 | 27.21 |
| 495 | 14.9 | 30.10 | 1181.7 | 465.40 | 23.80 |
| 495 | 31.9 | 64.44 | 1181.7 | 202.30 | 15.20 |
| 252 | 26.2 | 103.97 | 1197.6 | 118.60 | 10.38 |
| 252 | 75.8 | 300.79 | 1197.6 | 28.10 | 3.89 |
| 252 | 76.0 | 301.59 | 1197.6 | 28.20 | 3.88 |
| 126.8 | 78.4 | 618.30 | 1242.4 | 12.90 | 1.99 |
| 126.8 | 125.7 | 991.32 | 1242.4 | 7.60 | 1.25 |
| 126.8 | 375.2 | 2958.99 | 1242.4 | 2.55 | 0.42 |
| 126.8 | 7.7 | 60.7 | 273.1 | 25.6 | 4.08 |
| 126.8 | 17.1 | 134.9 | 273.1 | 10.4 | 1.95 |
| 126.8 | 20.7 | 163.2 | 273.1 | 8.5 | 1.62 |
| 126.8 | 20.6 | 162.5 | 273.1 | 8.5 | 1.63 |
| 126.8 | 29.4 | 231.9 | 273.1 | 5.8 | 1.15 |
| 126.8 | 42.4 | 334.4 | 273.1 | 3.9 | 0.80 |
| 126.8 | 94.0 | 741.3 | 273.1 | 1.9 | 0.37 |
| 126.8 | 38.1 | 300.47 | 146.8 | 7.20 | 0.46 |
| 126.8 | 74.9 | 590.69 | 146.8 | 1.80 | 0.25 |
| 126.8 | 75.6 | 596.21 | 146.8 | 2.60 | 0.24 |
| 126.8 | 126.5 | 997.63 | 146.8 | 0.80 | 0.15 |
| 126.8 | 376.8 | 2971.61 | 146.8 | 0.20 | 0.05 |

**Table A.8. Single-solute MTBE adsorption isotherm without buffer on silicalite zeolite HiSiv 3000**

**Adsorbent Type: Zeolite ZSM-5/silicalite (HiSiv 3000)**
**Solvent: ultrapure water without buffer**
**Micropollutant: MTBE**

| Solvent Volume (mL) | Weight of Zeolite (mg) | Zeolite Conc. (mg/L) | Initial MTBE Conc. (µg/L) | MTBE Conc. (µg/L) | Qe (mg/g) |
|---|---|---|---|---|---|
| 495 | 4.8 | 9.70 | 1054.3 | 744.71 | 31.93 |
| 495 | 15.3 | 30.91 | 1054.3 | 358.77 | 22.50 |
| 495 | 30.2 | 61.01 | 1054.3 | 168.42 | 14.52 |
| 252 | 25.0 | 99.21 | 1072.7 | 94.74 | 9.86 |
| 252 | 75.5 | 299.60 | 1072.7 | 24.56 | 3.50 |
| 252 | 75.8 | 300.79 | 1072.7 | 24.56 | 3.48 |
| 126.8 | 75.0 | 591.48 | 1112.0 | 12.55 | 1.86 |
| 126.8 | 125.6 | 990.54 | 1112.0 | 7.00 | 1.12 |
| 126.8 | 377.3 | 2975.55 | 1112.0 | 2.20 | 0.37 |

**Table A.9. Single-solute MTBE adsorption isotherm on ZSM-5 zeolite H-MFI-90 ($H^+$ form)**

**Adsorbent Type: Zeolite ZSM-5 (H-MFI-90)**
**Solvent: buffered ultrapure water at pH 7.2**
**Micropollutant: MTBE**

| Solvent Volume (mL) | Weight of Zeolite (mg) | Zeolite Conc. (mg/L) | Initial MTBE Conc. (µg/L) | MTBE Conc. (µg/L) | Qe (mg/g) |
|---|---|---|---|---|---|
| 495 | 5.2 | 10.51 | 1144.1 | 908.5 | 22.43 |
| 495 | 15.5 | 31.31 | 1144.1 | 575.4 | 18.16 |
| 495 | 30.0 | 60.61 | 1144.1 | 264.7 | 14.51 |
| 252 | 24.5 | 97.22 | 1167.5 | 130.3 | 10.67 |
| 252 | 75.3 | 298.81 | 1167.5 | 41.9 | 3.77 |
| 252 | 74.7 | 296.43 | 1167.5 | 40.6 | 3.80 |
| 126.8 | 75.6 | 596.21 | 1232.7 | 18.9 | 2.04 |
| 126.8 | 126.2 | 995.27 | 1232.7 | 10.5 | 1.23 |
| 126.8 | 375.8 | 2963.72 | 1232.7 | 3.4 | 0.41 |

**Table A.10. Single-solute MTBE adsorption isotherm on ZSM-5 zeolite H-MFI-400 ($H^+$ form)**

**Adsorbent Type: Zeolite ZSM-5 (H-MFI-400)**
**Solvent: buffered ultrapure water at pH 7.2**
**Micropollutant: MTBE**

| Solvent Volume (mL) | Weight of Zeolite (mg) | Zeolite Conc. (mg/L) | Initial MTBE Conc. (µg/L) | MTBE Conc. (µg/L) | Qe (mg/g) |
|---|---|---|---|---|---|
| 495 | 4.9 | 9.90 | 1148.8 | 893.1 | 25.83 |
| 495 | 15.2 | 30.71 | 1148.8 | 533.3 | 20.05 |
| 495 | 29.8 | 60.20 | 1148.8 | 294.5 | 14.19 |
| 252 | 25.1 | 99.60 | 1185.2 | 176.7 | 10.13 |
| 252 | 76.3 | 302.78 | 1185.2 | 42.4 | 3.77 |
| 252 | 75.5 | 299.60 | 1185.2 | 41.3 | 3.82 |
| 126.8 | 75.3 | 593.85 | 1153.7 | 21.3 | 1.91 |
| 126.8 | 126.3 | 996.06 | 1153.7 | 11.5 | 1.15 |
| 126.8 | 375.1 | 2958.20 | 1153.7 | 3.7 | 0.39 |

**Table A.11. Single-solute MTBE adsorption isotherm on Beta zeolite CP811C-300**

**Adsorbent Type: Zeolite Beta (CP811C-300)**
**Solvent: buffered ultrapure water at pH 7.2**
**Micropollutant: MTBE**

| Solvent Volume (mL) | Weight of Zeolite (mg) | Zeolite Conc. (mg/L) | Initial MTBE Conc. (µg/L) | MTBE Conc. (µg/L) | Qe (mg/g) |
|---|---|---|---|---|---|
| 252 | 76.4 | 303.17 | 1237.3 | 821.3 | 1.37 |
| 126.8 | 76.2 | 600.95 | 1331.2 | 664.2 | 1.11 |
| 126.8 | 125.0 | 985.80 | 1331.2 | 468.0 | 0.88 |
| 126.8 | 375.6 | 2962.15 | 1331.2 | 174.3 | 0.39 |

**Table A.12. Single-solute MTBE adsorption isotherm on Mordenite zeolite HSZ690-HOA**

**Adsorbent Type: Zeolite Mordenite (HSZ690-HOA)**
**Solvent: buffered ultrapure water at pH 7.2**
**Micropollutant: MTBE**

| Solvent Volume (mL) | Weight of Zeolite (mg) | Zeolite Conc. (mg/L) | Initial MTBE Conc. (µg/L) | MTBE Conc. (µg/L) | Qe (mg/g) |
|---|---|---|---|---|---|
| 495 | 4.8 | 9.70 | 1115.2 | 925.3 | 19.59 |
| 495 | 15.3 | 30.91 | 1115.2 | 569.8 | 17.65 |
| 495 | 30.6 | 61.82 | 1115.2 | 317.7 | 12.90 |
| 252 | 24.8 | 98.41 | 1176.0 | 179.4 | 10.13 |
| 252 | 76.3 | 302.78 | 1176.0 | 31.9 | 3.78 |
| 252 | 75.3 | 298.81 | 1176.0 | 32.8 | 3.83 |
| 126.8 | 74.9 | 590.69 | 1236.9 | 13.9 | 2.07 |
| 126.8 | 126.2 | 995.27 | 1236.9 | 7.1 | 1.24 |
| 126.8 | 375.1 | 2958.20 | 1236.9 | 2.9 | 0.42 |
| 126.8 | 8.6 | 67.8 | 273.1 | 43.3 | 3.39 |
| 126.8 | 18.5 | 145.9 | 273.1 | 17.9 | 1.75 |
| 126.8 | 22.4 | 176.7 | 273.1 | 13.6 | 1.47 |
| 126.8 | 22.1 | 174.3 | 273.1 | 14.1 | 1.49 |
| 126.8 | 30.0 | 236.6 | 273.1 | 12.5 | 1.10 |
| 126.8 | 41.0 | 323.3 | 273.1 | 6.2 | 0.83 |
| 126.8 | 84.1 | 663.2 | 273.1 | 2.7 | 0.41 |
| 495 | 5.3 | 10.71 | 113.0 | 108.5 | 0.42 |
| 495 | 15.4 | 31.11 | 113.0 | 82.8 | 0.97 |
| 495 | 30.2 | 61.01 | 113.0 | 36.2 | 1.26 |
| 252 | 25.6 | 101.59 | 111.9 | 12.7 | 0.98 |
| 252 | 76.4 | 303.17 | 111.9 | 2.4 | 0.36 |
| 252 | 76.3 | 302.78 | 111.9 | 2.2 | 0.36 |
| 126.8 | 77.3 | 609.62 | 113.3 | 1.1 | 0.18 |
| 126.8 | 126.9 | 1000.79 | 113.3 | 0.6 | 0.11 |
| 126.8 | 378.7 | 2986.59 | 113.3 | 0.3 | 0.04 |

**Table A.13. Single-solute MTBE adsorption isotherm on carbonaceous resin Ambersorb 563**

**Adsorbent Type: Carbonaceous resin (Ambersorb 563)**
**Solvent: buffered ultrapure water at pH 7.2**
**Micropollutant: MTBE**

| Solvent Volume (mL) | Weight of Zeolite (mg) | Zeolite Conc. (mg/L) | Initial MTBE Conc. (µg/L) | MTBE Conc. (µg/L) | Qe (mg/g) |
|---|---|---|---|---|---|
| 495 | 5.0 | 10.10 | 1062.1 | 875.2 | 18.50 |
| 495 | 16.4 | 33.13 | 1062.1 | 504.5 | 16.83 |
| 495 | 30.0 | 60.61 | 1062.1 | 264.2 | 13.17 |
| 252 | 25.6 | 101.59 | 1080.8 | 142.9 | 9.23 |
| 252 | 77.4 | 307.14 | 1080.8 | 21.5 | 3.45 |
| 252 | 74.6 | 296.03 | 1080.8 | 22.1 | 3.58 |
| 126.8 | 75.1 | 592.27 | 1140.6 | 7.2 | 1.91 |
| 126.8 | 376.3 | 2967.67 | 1140.6 | 0.7 | 0.38 |

**Table A.14. Single-solute MTBE adsorption isotherm on coconut-shell-based activated carbon CC-602**

**Adsorbent Type: Coconut-shell-based activated carbon (CC-602)**
**Solvent: buffered ultrapure water at pH 7.2**
**Micropollutant: MTBE**

| Solvent Volume (mL) | Weight of Zeolite (mg) | Zeolite Conc. (mg/L) | Initial MTBE Conc. (µg/L) | MTBE Conc. (µg/L) | Qe (mg/g) |
|---|---|---|---|---|---|
| 493.87 | 5.10 | 10.33 | 1274.4 | 1119.2 | 15.03 |
| 493.87 | 14.90 | 30.17 | 1274.4 | 948.7 | 10.80 |
| 493.87 | 29.90 | 60.54 | 1274.4 | 777.5 | 8.21 |
| 250.87 | 25.50 | 101.65 | 1197.6 | 522.0 | 6.65 |
| 250.87 | 75.50 | 300.95 | 1197.6 | 170.3 | 3.41 |
| 250.87 | 75.60 | 301.35 | 1197.6 | 155.5 | 3.46 |
| 125.67 | 74.50 | 592.83 | 1241.7 | 70.1 | 1.98 |
| 125.67 | 125.00 | 994.68 | 1241.7 | 27.4 | 1.22 |
| 125.67 | 375.90 | 2991.19 | 1241.7 | 10.2 | 0.41 |

**Table A.15. Single-solute MTBE adsorption isotherm on coal-based activated carbon UC-830**

**Adsorbent Type: Coal-based activated carbon (UC-830)**
**Solvent: buffered ultrapure water at pH 7.2**
**Micropollutant: MTBE**

| Solvent Volume (mL) | Weight of Zeolite (mg) | Zeolite Conc. (mg/L) | Initial MTBE Conc. (µg/L) | MTBE Conc. (µg/L) | Qe (mg/g) |
|---|---|---|---|---|---|
| 493.87 | 5.20 | 10.53 | 1200.9 | 1087.1 | 10.81 |
| 493.87 | 30.30 | 61.35 | 1200.9 | 935.2 | 4.33 |
| 250.87 | 26.90 | 107.23 | 1185.6 | 808.4 | 3.52 |
| 250.87 | 77.10 | 307.33 | 1185.6 | 483.1 | 2.29 |
| 250.87 | 74.90 | 298.56 | 1185.6 | 459.8 | 2.43 |
| 125.67 | 75.40 | 599.99 | 1107.3 | 245.2 | 1.44 |
| 125.67 | 124.90 | 993.88 | 1107.3 | 136.2 | 0.98 |
| 125.67 | 377.30 | 3002.33 | 1107.3 | 25.7 | 0.36 |
| 126.80 | 18.6 | 146.7 | 273.1 | 103.8 | 1.15 |
| 126.80 | 26.3 | 207.4 | 273.1 | 77.5 | 0.94 |
| 126.80 | 45.3 | 357.3 | 273.1 | 46.3 | 0.63 |
| 126.80 | 45.6 | 359.6 | 273.1 | 45.3 | 0.63 |
| 126.80 | 74.0 | 583.6 | 273.1 | 24.3 | 0.43 |
| 126.80 | 190.8 | 1504.7 | 273.1 | 6.2 | 0.18 |
| 126.80 | 230.6 | 1818.6 | 273.1 | 5.2 | 0.15 |
| 126.80 | 334.3 | 2636.4 | 273.1 | 3.1 | 0.10 |
| 126.80 | 503.6 | 3971.6 | 273.1 | 1.9 | 0.07 |

## Appendix B. Raw data for MTBE isotherms in the presence of co-adsorbing NOM

### Table B.1. MTBE adsorption isotherm in the presence of co-adsorbing NOM on zeolite ZSM-5 CBV 28014 ($NH_4^+$ form)

**Adsorbent Type: Zeolite ZSM-5 (CBV 28014)**
**Solvent: Tar River at water pH 7.6**
**Micropollutant: MTBE**

| Solvent Volume (mL) | Weight of Zeolite (mg) | Zeolite Conc. (mg/L) | Initial MTBE Conc. (µg/L) | MTBE Conc. (µg/L) | Qe (mg/g) |
|---|---|---|---|---|---|
| 495 | 5.3 | 10.71 | 108.5 | 49.7 | 5.49 |
| 495 | 14.7 | 29.70 | 108.5 | 24.2 | 2.84 |
| 495 | 29.0 | 58.59 | 108.5 | 12.3 | 1.64 |
| 252 | 24.8 | 98.41 | 116.5 | 7.2 | 1.11 |
| 252 | 74.5 | 295.63 | 116.5 | 2.4 | 0.39 |
| 252 | 75.7 | 300.40 | 116.5 | 2.3 | 0.38 |
| 126.8 | 79.2 | 624.61 | 125.9 | 1.2 | 0.20 |
| 126.8 | 128.2 | 1011.04 | 125.9 | 0.7 | 0.12 |
| 126.8 | 374.8 | 2955.84 | 125.9 | 0.3 | 0.04 |

### Table B.2. MTBE adsorption isotherm in the presence of co-adsorbing NOM on zeolite ZSM-5 SN-300 ($Na^+$ form)

**Adsorbent Type: Zeolite ZSM-5 (SN-300)**
**Solvent: Tar River water at pH 7.6**
**Micropollutant: MTBE**

| Solvent Volume (mL) | Weight of Zeolite (mg) | Zeolite Conc. (mg/L) | Initial MTBE Conc. (µg/L) | MTBE Conc. (µg/L) | Qe (mg/g) |
|---|---|---|---|---|---|
| 495 | 6.3 | 12.7 | 110.9 | 40.49 | 5.54 |
| 495 | 16.1 | 32.5 | 110.9 | 20.90 | 2.77 |
| 495 | 30.0 | 60.6 | 110.9 | 12.40 | 1.63 |
| 252 | 26.4 | 104.8 | 122.0 | 7.10 | 1.10 |
| 252 | 77.3 | 306.7 | 122.0 | 2.20 | 0.39 |
| 252 | 77.0 | 305.6 | 122.0 | 2.40 | 0.39 |
| 126.8 | 74.5 | 587.5 | 124.7 | 1.25 | 0.21 |
| 126.8 | 126.4 | 996.8 | 124.7 | 0.70 | 0.12 |
| 126.8 | 377.5 | 2977.1 | 124.7 | 0.30 | 0.04 |

**Table B.3. MTBE adsorption isotherm in the presence of co-adsorbing NOM on zeolite ZSM-5 H-MFI-240 ($H^+$ form)**

**Adsorbent Type: Zeolite ZSM-5 (H-MFI-240)**
**Solvent: Tar River water at pH 7.6**
**Micropollutant: MTBE**

| Solvent Volume (mL) | Weight of Zeolite (mg) | Zeolite Conc. (mg/L) | Initial MTBE Conc. (µg/L) | MTBE Conc. (µg/L) | Qe (mg/g) |
|---|---|---|---|---|---|
| 495 | 5.3 | 10.71 | 113.8 | 64.6 | 4.59 |
| 495 | 14.8 | 29.90 | 113.8 | 32.9 | 2.71 |
| 495 | 30.4 | 61.41 | 113.8 | 17.7 | 1.56 |
| 252 | 26.7 | 105.95 | 113.9 | 11 | 0.97 |
| 252 | 75.3 | 298.81 | 113.9 | 3.8 | 0.37 |
| 252 | 75.4 | 299.21 | 113.9 | 3.7 | 0.37 |
| 126.8 | 77.8 | 613.56 | 118.9 | 1.9 | 0.19 |
| 126.8 | 125.7 | 991.32 | 118.9 | 1.2 | 0.12 |
| 126.8 | 378.0 | 2981.07 | 118.9 | 0.4 | 0.04 |

**Table B.4. MTBE adsorption isotherm in the presence of co-adsorbing NOM on silicalite zeolite HiSiv 3000**

**Adsorbent Type: Zeolite ZSM-5/silicalite (HiSiv 3000)**
**Solvent: Tar River water at pH 7.6**
**Micropollutant: MTBE**

| Solvent Volume (mL) | Weight of Zeolite (mg) | Zeolite Conc. (mg/L) | Initial MTBE Conc. (µg/L) | MTBE Conc. (µg/L) | Qe (mg/g) |
|---|---|---|---|---|---|
| 495 | 5.6 | 11.31 | 124.7 | 76.5 | 4.26 |
| 495 | 14.7 | 29.70 | 124.7 | 33.5 | 3.07 |
| 495 | 32.5 | 65.66 | 124.7 | 11.6 | 1.72 |
| 252 | 24.8 | 98.41 | 112.8 | 7.3 | 1.07 |
| 252 | 75.3 | 298.81 | 112.8 | 2.2 | 0.37 |
| 252 | 75.5 | 299.60 | 112.8 | 2.2 | 0.37 |
| 126.8 | 75.3 | 593.85 | 124.9 | 1.2 | 0.21 |
| 126.8 | 125.9 | 992.90 | 124.9 | 0.7 | 0.13 |
| 126.8 | 376.2 | 2966.88 | 124.9 | 0.2 | 0.04 |

**Table B.5. MTBE adsorption isotherm in the presence of co-adsorbing NOM on zeolite Mordenite HSZ690-HOA**

**Adsorbent Type: Zeolite Mordenite (HSZ690-HOA)**
**Solvent: Tar River water at pH 7.6**
**Micropollutant: MTBE**

| Solvent Volume (mL) | Weight of Zeolite (mg) | Zeolite Conc. (mg/L) | Initial MTBE Conc. (µg/L) | MTBE Conc. (µg/L) | Qe (mg/g) |
|---|---|---|---|---|---|
| 495 | 5.2 | 10.51 | 121.8 | 101.9 | 1.89 |
| 495 | 15.4 | 31.11 | 121.8 | 70.3 | 1.66 |
| 495 | 30.5 | 61.62 | 121.8 | 31.9 | 1.46 |
| 252 | 27.4 | 108.73 | 123.0 | 11.3 | 1.03 |
| 252 | 75.2 | 298.41 | 123.0 | 2.0 | 0.41 |
| 252 | 74.9 | 297.22 | 123.0 | 2.0 | 0.41 |
| 126.8 | 75.8 | 597.79 | 125.0 | 0.9 | 0.21 |
| 126.8 | 126.3 | 996.06 | 125.0 | 0.5 | 0.12 |
| 126.8 | 377.4 | 2976.34 | 125.0 | 0.2 | 0.04 |

**Table B.6. MTBE adsorption isotherm in the presence of co-adsorbing NOM on carbonaceous resin Ambersorb 563**

**Adsorbent Type: Carbonaceous resin (Ambersorb 563)**
**Solvent: Tar River water at pH 7.6**
**Micropollutant: MTBE**

| Solvent Volume (mL) | Weight of Zeolite (mg) | Zeolite Conc. (mg/L) | Initial MTBE Conc. (µg/L) | MTBE Conc. (µg/L) | Qe (mg/g) |
|---|---|---|---|---|---|
| 495 | 5.2 | 10.51 | 105.9 | 63.34 | 4.05 |
| 495 | 14.6 | 29.49 | 105.9 | 24.10 | 2.77 |
| 495 | 30.7 | 62.02 | 105.9 | 7.40 | 1.59 |
| 252 | 25.9 | 102.78 | 101.1 | 3.80 | 0.95 |
| 252 | 75.5 | 299.60 | 101.1 | 0.90 | 0.33 |
| 252 | 76.4 | 303.17 | 101.1 | 1.00 | 0.33 |

**Table B.7. MTBE adsorption isotherm in the presence of co-adsorbing NOM on coconut-shell-based activated carbon CC-602**

**Adsorbent Type: Coconut-shell-based activated carbon (CC-602)**
**Solvent: Tar River water at pH 7.6**
**Micropollutant: MTBE**

| Solvent Volume (mL) | Weight of Zeolite (mg) | Zeolite Conc. (mg/L) | Initial MTBE Conc. (µg/L) | MTBE Conc. (µg/L) | Qe (mg/g) |
|---|---|---|---|---|---|
| 493.87 | 5.10 | 10.33 | 107.3 | 92.7 | 1.41 |
| 493.87 | 15.10 | 30.57 | 107.3 | 73.9 | 1.09 |
| 493.87 | 31.60 | 63.98 | 107.3 | 47.9 | 0.93 |
| 250.87 | 25.10 | 100.05 | 104.0 | 33.0 | 0.71 |
| 250.87 | 76.50 | 304.94 | 104.0 | 7.4 | 0.32 |
| 250.87 | 75.20 | 299.76 | 104.0 | 8.5 | 0.32 |
| 125.67 | 77.40 | 615.90 | 107.6 | 4.6 | 0.17 |
| 125.67 | 127.20 | 1012.18 | 107.6 | 1.5 | 0.10 |
| 125.67 | 374.80 | 2982.44 | 107.6 | 0.6 | 0.04 |

**Table B.8. MTBE adsorption isotherm in the presence of co-adsorbing NOM on coal-based activated carbon UC-830**

**Adsorbent Type: Coal-based activated carbon (UC-830)**
**Solvent: Tar River water at pH 7.6**
**Micropollutant: MTBE**

| Solvent Volume (mL) | Weight of Zeolite (mg) | Zeolite Conc. (mg/L) | Initial MTBE Conc. (µg/L) | MTBE Conc. (µg/L) | Qe (mg/g) |
|---|---|---|---|---|---|
| 493.87 | 4.90 | 9.92 | 100.8 | 95.0 | 0.58 |
| 493.87 | 30.70 | 62.16 | 100.8 | 79.3 | 0.35 |
| 250.87 | 25.60 | 102.05 | 101.2 | 72.5 | 0.28 |
| 250.87 | 78.00 | 310.92 | 101.2 | 40.8 | 0.19 |
| 250.87 | 78.00 | 310.92 | 101.2 | 42.4 | 0.19 |
| 125.67 | 75.30 | 599.19 | 99.8 | 12.3 | 0.15 |
| 125.67 | 124.90 | 993.88 | 99.8 | 6.4 | 0.09 |
| 125.67 | 376.90 | 2999.15 | 99.8 | 1.8 | 0.03 |

**Table B.9. MTBE adsorption isotherm in the presence of co-adsorbing NOM on coal-based activated carbon F600**

**Adsorbent Type: Coal-based activated carbon (F600)**
**Solvent: Tar River water at pH 7.6**
**Micropollutant: MTBE**

| Solvent Volume (mL) | Weight of Zeolite (mg) | Zeolite Conc. (mg/L) | Initial MTBE Conc. (µg/L) | MTBE Conc. (µg/L) | Qe (mg/g) |
|---|---|---|---|---|---|
| 493.87 | 5.00 | 10.12 | 109.3 | 102.9 | 0.63 |
| 493.87 | 15.40 | 31.18 | 109.3 | 87.6 | 0.70 |
| 493.87 | 30.60 | 61.96 | 109.3 | 66.2 | 0.70 |
| 250.87 | 25.00 | 99.65 | 105.0 | 52.7 | 0.53 |
| 250.87 | 75.90 | 302.55 | 105.0 | 18.0 | 0.29 |
| 250.87 | 76.00 | 302.95 | 105.0 | 18.8 | 0.28 |
| 125.67 | 75.50 | 600.78 | 107.0 | 8.5 | 0.16 |
| 125.67 | 125.10 | 995.47 | 107.0 | 4.5 | 0.10 |
| 125.67 | 374.90 | 2983.23 | 107.0 | 1.3 | 0.04 |

## Appendix C. Raw data for MTBE isotherms in the presence of preloaded NOM

**Table C.1. MTBE adsorption isotherm in the presence of preloaded NOM on zeolite ZSM-5 CBV 28014 ($NH_4^+$ form)**

**Adsorbent Type: Zeolite ZSM-5 (CBV 28014)**
**Solvent: Tar River water at pH 7.6**
**Micropollutant: MTBE**

| Solvent Volume (mL) | Weight of Zeolite (mg) | Zeolite Conc. (mg/L) | Initial MTBE Conc. (µg/L) | MTBE Conc. (µg/L) | Qe (mg/g) |
|---|---|---|---|---|---|
| 495 | 4.7 | 9.49 | 142.7 | 62.8 | 8.40 |
| 495 | 15.1 | 30.51 | 142.7 | 26.4 | 3.81 |
| 495 | 29.9 | 60.40 | 142.7 | 13.3 | 2.14 |
| 252 | 25.0 | 99.21 | 143.3 | 8.7 | 1.36 |
| 252 | 76.3 | 302.78 | 143.3 | 2.9 | 0.46 |
| 252 | 76.0 | 301.59 | 143.3 | 2.9 | 0.47 |
| 126.8 | 75.3 | 593.85 | 153.0 | 1.7 | 0.25 |
| 126.8 | 127.0 | 1001.58 | 153.0 | 1.0 | 0.15 |
| 126.8 | 375.9 | 2964.51 | 153.0 | 0.3 | 0.05 |

**Table C.2. MTBE adsorption isotherm in the presence of preloaded NOM on zeolite ZSM-5 SN-300 ($Na^+$ form)**

**Adsorbent Type: Zeolite ZSM-5 (SN-300)**
**Solvent: Tar River water at pH 7.6**
**Micropollutant: MTBE**

| Solvent Volume (mL) | Weight of Zeolite (mg) | Zeolite Conc. (mg/L) | Initial MTBE Conc. (µg/L) | MTBE Conc. (µg/L) | Qe (mg/g) |
|---|---|---|---|---|---|
| 495 | 4.5 | 9.09 | 142.7 | 72.3 | 7.73 |
| 495 | 15.1 | 30.51 | 142.7 | 28.6 | 3.74 |
| 495 | 29.6 | 59.80 | 142.7 | 15.1 | 2.13 |
| 252 | 25.0 | 99.21 | 143.3 | 9.3 | 1.35 |
| 252 | 75.0 | 297.62 | 143.3 | 3.1 | 0.47 |
| 252 | 75.7 | 300.40 | 143.3 | 2.9 | 0.47 |
| 126.8 | 76.8 | 605.68 | 153.0 | 1.7 | 0.25 |
| 126.8 | 125.0 | 985.80 | 153.0 | 1.3 | 0.15 |
| 126.8 | 375.7 | 2962.93 | 153.0 | 0.6 | 0.05 |

**Table C.3. MTBE adsorption isotherm in the presence of preloaded NOM on zeolite ZSM-5 H-MFI-240 ($H^+$ form)**

**Adsorbent Type: Zeolite ZSM-5 (H-MFI-240)**
**Solvent: Tar River water at pH 7.6**
**Micropollutant: MTBE**

| Solvent Volume (mL) | Weight of Zeolite (mg) | Zeolite Conc. (mg/L) | Initial MTBE Conc. (µg/L) | MTBE Conc. (µg/L) | Qe (mg/g) |
|---|---|---|---|---|---|
| 495 | 4.9 | 9.90 | 142.7 | 80.1 | 6.32 |
| 495 | 14.9 | 30.10 | 142.7 | 37.8 | 3.48 |
| 495 | 30.2 | 61.01 | 142.7 | 19.6 | 2.02 |
| 252 | 24.8 | 98.41 | 143.3 | 13.1 | 1.32 |
| 252 | 75.3 | 298.81 | 143.3 | 4.1 | 0.47 |
| 252 | 75.9 | 301.19 | 143.3 | 4.0 | 0.46 |
| 126.8 | 74.8 | 589.91 | 153.0 | 2.2 | 0.26 |
| 126.8 | 125.0 | 985.80 | 153.0 | 1.3 | 0.15 |
| 126.8 | 374.9 | 2956.62 | 153.0 | 0.4 | 0.05 |

**Table C.4. MTBE adsorption isotherm in the presence of preloaded NOM on silicalite zeolite HiSiv 3000**

**Adsorbent Type: Zeolite ZSM-5/silicalite (HiSiv 3000)**
**Solvent: Tar River water at pH 7.6**
**Micropollutant: MTBE**

| Solvent Volume (mL) | Weight of Zeolite (mg) | Zeolite Conc. (mg/L) | Initial MTBE Conc. (µg/L) | MTBE Conc. (µg/L) | Qe (mg/g) |
|---|---|---|---|---|---|
| 495 | 14.9 | 30.10 | 132.7 | 32.8 | 3.32 |
| 495 | 30.0 | 60.61 | 132.7 | 14.7 | 1.95 |
| 252 | 25.5 | 101.19 | 132.7 | 9.0 | 1.22 |
| 252 | 75.0 | 297.62 | 132.7 | 2.7 | 0.44 |
| 252 | 75.0 | 297.62 | 132.7 | 2.7 | 0.44 |
| 126.8 | 75.7 | 597.00 | 136.4 | 1.3 | 0.23 |
| 126.8 | 125.3 | 988.17 | 136.4 | 0.8 | 0.14 |
| 126.8 | 375.8 | 2963.72 | 136.4 | 0.2 | 0.05 |

**Table C.5. MTBE adsorption isotherm in the presence of preloaded NOM on zeolite Mordenite HSZ690-HOA**

**Adsorbent Type: Zeolite Mordenite (HSZ690-HOA)**
**Solvent: Tar River water at pH 7.6**
**Micropollutant: MTBE**

| Solvent Volume (mL) | Weight of Zeolite (mg) | Zeolite Conc. (mg/L) | Initial MTBE Conc. (µg/L) | MTBE Conc. (µg/L) | Qe (mg/g) |
|---|---|---|---|---|---|
| 495 | 4.7 | 9.49 | 117.2 | 112.7 | 0.47 |
| 495 | 15.0 | 30.30 | 117.2 | 84.9 | 1.07 |
| 495 | 30.2 | 61.01 | 117.2 | 31.0 | 1.41 |
| 252 | 25.1 | 99.60 | 122.0 | 14.4 | 1.08 |
| 252 | 74.8 | 296.83 | 122.0 | 1.9 | 0.40 |
| 252 | 75.4 | 299.21 | 122.0 | 2.0 | 0.40 |
| 126.8 | 77.3 | 609.62 | 115.8 | 0.8 | 0.19 |
| 126.8 | 125.2 | 987.38 | 115.8 | 0.5 | 0.12 |
| 126.8 | 375.8 | 2963.72 | 115.8 | 0.2 | 0.04 |

**Table C.6. MTBE adsorption isotherm in the presence of preloaded NOM on carbonaceous resin Ambersorb 563**

**Adsorbent Type: Carbonaceous resin (Ambersorb 563)**
**Solvent: Tar River water at pH 7.6**
**Micropollutant: MTBE**

| Solvent Volume (mL) | Weight of Zeolite (mg) | Zeolite Conc. (mg/L) | Initial MTBE Conc. (µg/L) | MTBE Conc. (µg/L) | Qe (mg/g) |
|---|---|---|---|---|---|
| 493.87 | 5.0 | 10.12 | 126.6 | 110.7 | 1.57 |
| 493.87 | 14.9 | 30.17 | 126.6 | 51.0 | 2.51 |
| 493.87 | 29.7 | 60.14 | 126.6 | 18.3 | 1.80 |
| 250.87 | 24.9 | 99.25 | 125.1 | 9.2 | 1.17 |
| 250.87 | 75.1 | 299.36 | 125.1 | 2.5 | 0.41 |
| 250.87 | 75.7 | 301.75 | 125.1 | 1.7 | 0.41 |
| 125.67 | 75.3 | 599.19 | 130.2 | 0.8 | 0.22 |
| 125.67 | 126.5 | 1006.61 | 130.2 | 0.6 | 0.13 |
| 125.67 | 376.6 | 2996.76 | 130.2 | 0.6 | 0.04 |

**Table C.7. MTBE adsorption isotherm in the presence of preloaded NOM on coconut-shell-based activated carbon CC-602**

**Adsorbent Type: Coconut-shell-based activated carbon (CC-602)**
**Solvent: Tar River water at pH 7.6**
**Micropollutant: MTBE**

| Solvent Volume (mL) | Weight of Zeolite (mg) | Zeolite Conc. (mg/L) | Initial MTBE Conc. (µg/L) | MTBE Conc. (µg/L) | Qe (mg/g) |
|---|---|---|---|---|---|
| 493.87 | 14.70 | 29.76 | 132.8 | 96.6 | 1.22 |
| 493.87 | 30.60 | 61.96 | 132.8 | 65.1 | 1.09 |
| 250.87 | 25.90 | 103.24 | 128.7 | 43.5 | 0.83 |
| 250.87 | 76.00 | 302.95 | 128.7 | 7.4 | 0.40 |
| 250.87 | 75.70 | 301.75 | 128.7 | 10.3 | 0.39 |
| 125.67 | 76.60 | 609.54 | 140.6 | 4.2 | 0.22 |
| 125.67 | 125.90 | 1001.84 | 140.6 | 2.2 | 0.14 |
| 125.67 | 376.60 | 2996.76 | 140.6 | 0.7 | 0.05 |

**Table C.8. MTBE adsorption isotherm in the presence of preloaded NOM on coal-based activated carbon UC-830**

**Adsorbent Type: Coal-based activated carbon (UC-830)**
**Solvent: Tar River water at pH 7.6**
**Micropollutant: MTBE**

| Solvent Volume (mL) | Weight of Zeolite (mg) | Zeolite Conc. (mg/L) | Initial MTBE Conc. (µg/L) | MTBE Conc. (µg/L) | Qe (mg/g) |
|---|---|---|---|---|---|
| 493.87 | 5.0 | 10.12 | 128.4 | 120.3 | 0.80 |
| 493.87 | 15.7 | 31.79 | 128.4 | 116.0 | 0.39 |
| 493.87 | 29.9 | 60.54 | 128.4 | 107.6 | 0.34 |
| 250.87 | 25.3 | 100.85 | 134.2 | 94.8 | 0.39 |
| 250.87 | 75.7 | 301.75 | 134.2 | 36.8 | 0.32 |
| 250.87 | 74.3 | 296.17 | 134.2 | 37.8 | 0.33 |
| 125.67 | 72.2 | 574.53 | 138.1 | 17.5 | 0.21 |
| 125.67 | 125.8 | 1001.04 | 138.1 | 8.4 | 0.13 |
| 125.67 | 376.5 | 2995.96 | 138.1 | 1.9 | 0.05 |

**Table C.9. MTBE adsorption isotherm in the presence of preloaded NOM on coal-based activated carbon F600**

**Adsorbent Type: Coal-based activated carbon (F600)**
**Solvent: Tar River water at pH 7.6**
**Micropollutant: MTBE**

| Solvent Volume (mL) | Weight of Zeolite (mg) | Zeolite Conc. (mg/L) | Initial MTBE Conc. (µg/L) | MTBE Conc. (µg/L) | Qe (mg/g) |
|---|---|---|---|---|---|
| 493.87 | 15.5 | 31.38 | 132.9 | 108.7 | 0.77 |
| 493.87 | 30.8 | 62.36 | 132.9 | 92.1 | 0.65 |
| 250.87 | 26.3 | 104.84 | 135.9 | 67.5 | 0.65 |
| 250.87 | 74.8 | 298.16 | 135.9 | 26.9 | 0.37 |
| 250.87 | 75.6 | 301.35 | 135.9 | 25.8 | 0.37 |
| 125.67 | 75.4 | 599.99 | 142.0 | 12.8 | 0.22 |
| 125.67 | 125.6 | 999.45 | 142.0 | 6.6 | 0.14 |
| 125.67 | 376.4 | 2995.17 | 142.0 | 2.0 | 0.05 |